

Morphological insights from Ecology and Evolution: Mandibular plasticity and phenotypic variation in Cervini from different populations and contrasted habitats

Emilie Berlioz^{1,2}, Raúl Torres-Román³, Araceli Gort-Esteve⁴, Mariano L. Merino⁵, Vebjørn Veiberg⁶, Concepción Azorit Casas³

¹Research group I+D+i EvoAdapta (Evolución Humana y Adaptaciones durante La Prehistoria), Dpt. of Historical Sciences, University of Cantabria, Santander, Spain

²Laboratoire PALEVOPRIM (Paleontology Evolution Paleoecosystems Paleoprimatology), UMR 7262, CNRS & Université de Poitiers, France

³Research group PAIDI RNM175 (Biodiversidad y Desarrollo Sostenible), Dpt. Animal Biology, Plant Biology and Ecology, Universidad de Jaén, 23071 Jaén

⁴Institute for Game and Wildlife Research, IREC (CSIC-UCLM-JCCM), 13005 Ciudad Real

⁵Universidad Nacional del Noroeste de la Provincia de Buenos Aires, Pergamino, Buenos Aires, Argentina. Comisión de Investigaciones Científicas de la Provincia de Buenos Aires

⁶Norwegian Institute for Nature Research, P.O. Box 5685 Sluppen, NO-7485 Trondheim

Emilie Berlioz -  [0000-0002-2694-8436](https://orcid.org/0000-0002-2694-8436)

Raúl Torres-Román -  [0000-0003-1053-3161](https://orcid.org/0000-0003-1053-3161)

Araceli Gort-Esteve -  [0000-0003-1894-9006](https://orcid.org/0000-0003-1894-9006)

Vebjørn Veiberg -  [0000-0003-1037-5183](https://orcid.org/0000-0003-1037-5183)

Concepción Azorit Casas -  [0000-0001-9538-7110](https://orcid.org/0000-0001-9538-7110)

Abstract:

Understanding how genetic variations and environmental constraints influence morphological differences is crucial to interpreting phenotypic diversity. The mandible is a key structure widely used to make inferences about feeding ecology and habitat conditions in early ungulate growth. However, most studies focus on interspecific comparisons, and few address mandibular plasticity and variations at inter- and intrapopulation scales. In this study, we used a 2D geometric-morphometric approach to analyse how these factors shape the mandibles of two Cervini species characterised by different contexts, populations and belonging to distinct lineages: the red deer (*Cervus elaphus*) and the rusa deer (*Rusa timorensis*).

For the European red deer, we found clear variations in mandibular morphology along a north-south transect from Norway to southern Spain. These variations are related to the need for different biomechanical forces to masticate vegetal resources with distinct physical properties, under contrasting climates. The mandibles of red deer in southern Europe are more robust, probably due to the higher proportion of highly fibrous, tough herbaceous monocotyledons in their diet. In contrast, northern populations have slender mandibles, reflecting the consumption of a softer diet. The American population of red deer from Argentina shows a different trend, both in size and shape.

A recent study showed that New Caledonian rusa deer constituted a single genetic population. Here, we identified significant intrapopulation differences between contrasting local habitats. Gouaro-Déva rusa deer are significantly smaller, which we interpret as the consequence of greater stress, impacting the growth and ontogenic development of these animals. Deer from tropical forests have a more robust mandible than in grassy areas, aligning with the biomechanical needs of their respective diets.

Morphological variations in deer jaws at intraspecific and interspecific scales provide insights into the ecology and environment of these animals, and offer potential for future (paleo)ecological research using geometric morphometric approaches.

Keywords: geometric morphometrics, environmental constraints, ecological plasticity, Cervini, (eco-)Phenotype.

Received: 2025-02-16

Revised: 2025-02-22

Accepted: 2025-02-23

Short title

Mandibular Plasticity and Variation in Cervini

Corresponding author

Emilie Berlioz

Research group I+D+i EvoAdapta (Evolución Humana y Adaptaciones durante La Prehistoria), Dpt. of Historical Sciences, University of Cantabria, Santander, Spain; email: emilieberliozpro@gmail.com

Phone: +33625341278

1 1 **Morphological insights from Ecology and Evolution: Mandibular plasticity and**
2 2 **phenotypic variation in Cervini from different populations and contrasted habitats**

3
4
5 5 Running title:

6 6 **Mandibular Plasticity and Variation in Cervini**

7 7 Abstract

8 8 Understanding how genetic variations and environmental constraints influence morphological
9 9 differences is crucial to interpreting phenotypic diversity. The mandible is a key structure widely
10 10 used to make inferences about feeding ecology and habitat conditions in early ungulate growth.
11 11 However, most studies focus on interspecific comparisons, and few address mandibular
12 12 plasticity and variations at inter- and intrapopulation scales. In this study, we used a 2D
13 13 geometric-morphometric approach to analyse how these factors shape the mandibles of two
14 14 *Cervini* species characterised by different contexts, populations and belonging to distinct
15 15 lineages: the red deer (*Cervus elaphus*) and the rusa deer (*Rusa timorensis*).

16 16 For the European red deer, we found clear variations in mandibular morphology along a north-
17 17 south transect from Norway to southern Spain. These variations are related to the need for
18 18 different biomechanical forces to masticate vegetal resources with distinct physical properties,
19 19 under contrasting climates. The mandibles of red deer in southern Europe are more robust,
20 20 probably due to the higher proportion of highly fibrous, tough herbaceous monocotyledons in
21 21 their diet. In contrast, northern populations have slender mandibles, reflecting the consumption
22 22 of a softer diet. The American population of red deer from Argentina shows a different trend,
23 23 both in size and shape.

24 24 A recent study showed that New Caledonian rusa deer constituted a single genetic population.
25 25 Here, we identified significant intrapopulation differences between contrasting local habitats.
26 26 >Gouaro-Déva rusa deer are significantly smaller, which we interpret as the consequence of
27 27 greater stress, impacting the growth and ontogenic development of these animals. Deer from
28 28 tropical forests have a more robust mandible than in grassy areas, aligning with the
29 29 biomechanical needs of their respective diets.

31 30 Morphological variations in deer jaws at intraspecific and interspecific scales provide insights
32 31 into the ecology and environment of these animals, and offer potential for future
33 32 (paleo)ecological research using geometric morphometric approaches.

34 33 **Keywords**

35 34 Cervini, (eco-)Phenotype, environmental constraints, ecological plasticity, geometric
36 35 morphometrics

37 36

Introduction

Understanding the relationship and interactions between environmental factors and historical contingencies is a classic question in evolutionary biology. It is essential for elucidating how populations interact and respond to their habitats and the underlying processes behind phenotypic diversity. As stated by Seilacher (1970), morphology is shaped by a combination of genetic inheritance, structural constraints and environmental adaptations. This framework provides a solid theoretical basis for studying how these three factors interact.

Mandible morphology is a key functional trait closely related to animal diet. Its highly plastic tissue is constantly remodelled by the functional stresses it undergoes (Currey, 2003; Wolff, 1892). Among the factors influencing mandibular morphology, the mechanical forces acting during mastication in response to the hardness, toughness or size of ingested particles play a significant role (Clauss et al., 2008; Fletcher et al., 2010; Janis, 1995; Paschetta et al., 2010; Varela and Fariña, 2015; Wang et al., 2022). After a change in diet, a few months can be enough to detect significant differences in shape (Neaux et al., 2022). As a result, the morphology of the mandible provides valuable ecological information, particularly on diet (De Felice et al., 2020; Neaux et al., 2022, 2021; Spencer, 1995). However, most studies investigating the relationship between mandible morphology and feeding ecology focus on interspecific comparisons, emphasizing the significant impact of phylogenetic affinities compared with that of adaptation to available resources in the habitat (Fletcher et al., 2010; Pérez-Barbería and Gordon, 1999; Raia et al., 2010; Zhou et al., 2019). There are comparatively few studies addressing these issues at both inter- and intrapopulation scales (Kangas et al., 2017; Ozaki et al., 2007), although several ungulate species provide good candidates, with their wide geographical distribution and well-known ecological plasticity.

In this study, based on a 2D geometric morphometric approach, we aim to contribute to filling this gap by investigating how genetic variants and environmental constraints affect the mandibular bone morphology of the red deer *Cervus elaphus* and the rusa deer *Rusa timorensis*,

66 63 two *Cervini* species characterised by different contexts and belonging to distinct lineages
67 64 (Mackiewicz et al., 2022).

68 65 *Cervus elaphus* dispersed in Europe during the middle Pleistocene (Croitor, 2018). The current
69 66 genetic structure of *Cervus elaphus* is divided into three main genetic lineages (western
70 67 European, eastern European, Mediterranean ; Niedziałkowska et al., 2011; Skog et al., 2009;
71 68 Zachos et al., 2016), resulting from the contraction of the distribution range of the species into
72 69 refugial areas during the last glacial maximum (Hewitt, 1999; Jones et al., 2020; Meiri et al.,
73 70 2013; Taberlet et al., 1998). Red deer populations originating from the Iberian glacial refuge
74 71 were the primary source of postglacial recolonisation and subspecific radiation in north-western
75 72 Europe (Carranza et al., 2016; Meiri et al., 2013). Northern Norway and Southern Spain
76 73 represent the extreme north and south of the European *Cervus elaphus* native distribution along
77 74 a clear bioclimatic gradient (Lovari et al., 2018). The species has also been introduced beyond
78 75 its native range, where it has often established successful and sometimes invasive populations,
79 76 for example, in Australia (Kelly et al., 2023), New Zealand (Latham and Nugent, 2017) or
80 77 Argentina (Novillo and Ojeda, 2008). This reflects its remarkable ecological plasticity (Azorit et
81 78 al., 2012; Bugalho and Milne, 2003; Gebert and Verheyden-Tixier, 2001; Geist, 1998). The wide
82 79 geographical distribution demonstrates its broad climatic tolerance and its ecological plasticity.
83 80 The well-documented genetic of *Cervus elaphus* makes it an excellent species for studying the
84 81 influence of genetic and environmental factors on mandibular bone morphology at an
85 82 interpopulation scale.

86 83 *Rusa timorensis* (Blainville, 1822) is endemic to the Indonesian islands of Bali and Java, where it
87 84 is considered vulnerable by the IUCN Red List (Hedges et al., 2008). There, it occupies a diversity
88 85 of habitats, from forests to grasslands. Its diet is adaptable, with a preference for herbaceous
89 86 monocotyledons (Hedges et al., 2008). In 1870, twelve rusa deer individuals were introduced to
90 87 New Caledonia, which now hosts the largest population of the species in the world (Savouré-
91 88 Soubelet et al., 2021). New Caledonia is a biodiversity hotspot (Mittermeier et al., 2011; Myers

93 89 et al., 2000) where the rusa deer is an exotic invasive species (Barrau and Devambe, 1957;
94 90 Gargominy et al., 1996). It is regarded by local institutions as a "natural disaster", because of the
95 91 major threat it poses to both agriculture and ecosystems. In New Caledonia, herbaceous
96 92 monocotyledons represent the major part of the diet of this cervid as soon as is available. However,
97 93 they are characterised by great dietary plasticity and are able to turn to alternative food
98 94 resources when this preferred resource is lacking (Berlioz et al., 2020, unpublished CNRS report).
99 95 This plasticity enables it to occupy a wide range of habitats. A recent study (Frantz et al., 2024)
100 96 revealed a unique, genetically homogeneous population throughout New Caledonia, while
101 97 empiric observations of local Neo-Caledonian hunters suggest animal size variations based on
102 98 geographic origin on the Grande Terre. This context offers a unique opportunity to explore the
103 99 mandibular bone morphological variation within a population in response to different
104 100 environments while breaking free from genetic influence.

105 101 This study aims to determine the relative importance of both genetic and environmental
106 102 factors in shaping *Cervini* mandibular bone morphology at the intraspecific scale. For *Cervus*
107 103 *elaphus*, we expect that an interaction between these two factors can explain the observed
108 104 morphological patterns, while *Rusa timorensis* is anticipated to respond to the characteristics of
109 105 local habitats. This study will also help better interpret mandibular morphological changes in
110 106 future paleoecological studies.

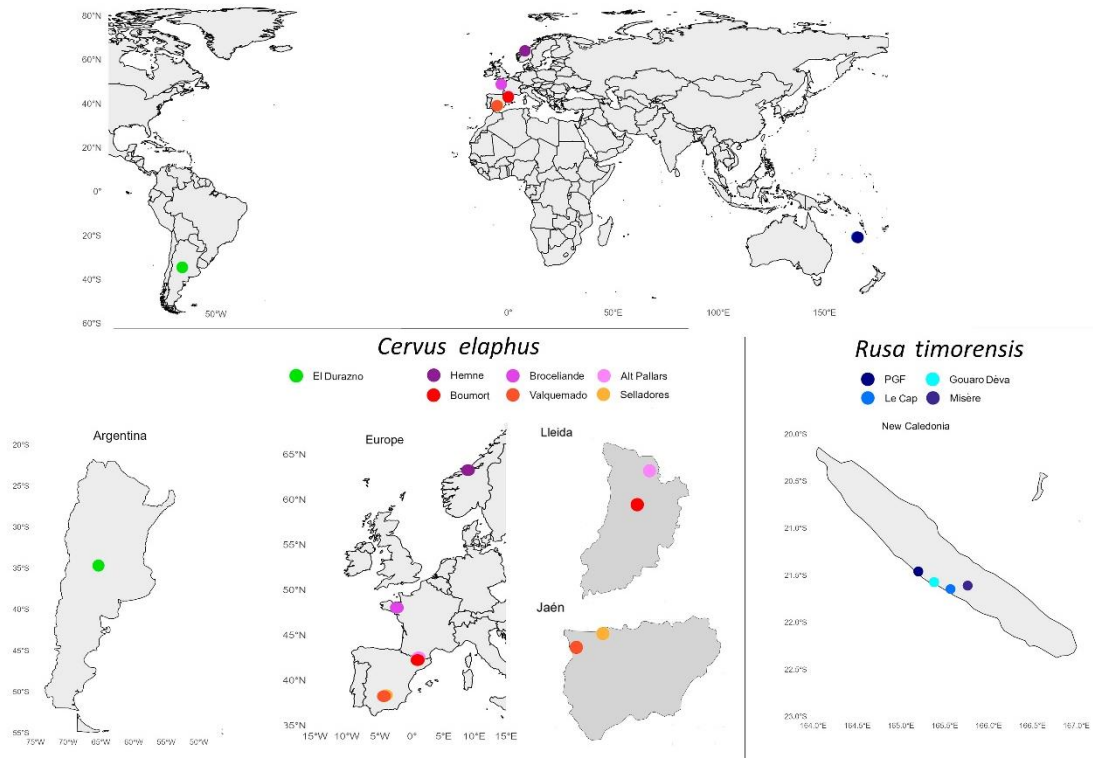
111 107

112 108 **Material and methods**

113 109 **Material**

114 110 These individuals belong to 8 populations of extant cervid species (7 populations of *Cervus*
115 111 *elaphus* and one of *Rusa timorensis*), with different genetic origins and contrasting habitats (Fig.
116 112 1). For most specimens, the sex and date of death are known, and the habitat is well-
117 113 characterized in all cases. To limit ontogenetic allometry's impact on shape variations, we
118 114 studied 315 hemi-mandibles of *Cervini*, focusing on adults with tooth eruption and dental wear

120 115 compatible with an age of more than 5-6 years old, when the mandibular growth is normally
 121 116 completed (Azorit et al., 2003).
 122 117



123 Figure 1: Location of the eight Cervini populations included in the study. *Cervus elaphus*: El Durazno, Hemne,
 124 Broceliande, Alt Pallars, Boumort, Selladores, Valquemado. The focus on the Lleida region gives a better view of the Alt
 125 Pallar and Boumort populations. The focus on Jaen area gives a better view of the Valquemado and Selladores
 126 populations. *Rusa timorensis*: New Caledonia (Gouaro Déva, Le Cap, Misère, Parc des Grandes Fougères (PGF)).

127 118 **Red deer material**

128 119 The red deer population of **El Durazno** (N= 21; Fig. 1) originates from a hunting ground located
 129 120 20 km north of Buena Esperanza in the Province of San Luis, Argentina (-34.5459; -65.2982) in
 130 121 the Pampa Ecoregion (Table 1). The area is a grassy steppe, primarily covered with tussock

122 bushes. It typically includes small groves of chañar trees (*Geoffroea decorticans*). In some places,
123 isolated caldén trees (*Prosopis caldenia*) are also present (Anderson et al., 1970).

134 **Table 1: Information on the habitats of cervid populations.** Information on biomes is taken from
135 <https://ecoregions.appspot.com/>. Description of the local vegetation for the populations living in geographical Europe is
136 taken from Ozenda and Borel, 2000. For El Durazno and the Neo-Caledonian localities, the description is based on field
137 observations.

| | Group | Biome | Local vegetation description |
|------------------------|---------------------------|--|--|
| <i>Cervus elaphus</i> | Alt Pallars | Temperate Broadleaf & Mixed Forests | High mountain: subalpine, alpine and nival vegetation belts |
| | Boumort | Temperate Broadleaf & Mixed Forests | Lower and mid-mountain: collinean and montane vegetation belts |
| | Broceliande (Paimpont) | Temperate Broadleaf & Mixed Forests | Hyperhygrophilous Armorican sector |
| | El Durazno | Temperate Grasslands, Savannas & Shrublands | Semiarid Pampas |
| | Hemne | Boreal Forests/Taiga | Orocaledonian vegetation unit (mountain tundra) |
| | Selladores | Mediterranean Forests, Woodlands & Scrub | Siliceous, with round-leaved oak |
| <i>Rusa timorensis</i> | Valquemado | Mediterranean Forests, Woodlands & Scrub | Calicolous, with round-leaved oak |
| | Gouaro Déva | Tropical & Subtropical Dry Broadleaf Forests | Sclerophyllous & meso-sclerophyll forests, extensive grasslands, Niaoulis savannah |
| | Le Cap | Tropical & Subtropical Dry Broadleaf Forests | Niaoulis savannah & agricultural grasslands |
| | Misère | Tropical & Subtropical Dry Broadleaf Forests | Mesophyll forest |
| | Parc des Grandes Fougères | Tropical & Subtropical Moist Broadleaf Forests | Dense tropical rainforest |

124
125 Mean annual precipitation is 510 mm, about 80% of which falls between October and April, with
126 low water availability during winter (Berton and Echeverría, 1999). The mean annual
127 temperature is 17°C, with a strong continental effect (43°C in summer and 15°C in winter;
128 Anderson, 1979). Although there is no data on the diet of *Cervus elaphus* in the southern portion
129 of the province of San Luis; there is data in the neighbour province of Pampa, where this deer
130 has 39.5% grasses in its annual diet (Pordomingo and Rucci, 2000). Specimens included in this
131 study were hunted between 2022 and 2023. The El Durazno population was introduced to
132 Argentina in 1904 (Novillo and Ojeda, 2008). Specimens came from various populations across
133 Eastern Europe, specifically Germany, Austria, and the Carpathian Mountains. Deer from Eastern
134 Europe represent a unique genetic lineage (Jaksic et al., 2002; Skog et al., 2009). In Argentina,
135 red deer are considered an invasive exotic species (Merino et al., 2009)
136 The western European populations of *Cervus elaphus* included in the present study all belong to
137 the Western European genetic lineage (Skog et al., 2009). This lineage is further structured
138 (Niedziałkowska et al., 2011; Zachos et al., 2016) with Iberian deer (*Cervus elaphus hispanicus*)
139 forming a genetically distinct group from the other western European populations among the
140 Western European lineage (Carranza et al., 2016).

156 141 The red deer population from the municipality of **Hemne** (N = 35; Fig. 1; Table 1) comes from
157 142 the southwest of Trøndelag county, in Mid-Norway (63.2885, 9.2157). The region is
158 143 characterized by areas with open coniferous forest under an oceanic climate in a low-altitude
159 144 coastal fjord landscape (Albon and Langvatn, 1992; Aune, 1973). The tree cover mainly consists
160 145 of Scots pine (*Pinus sylvestris*) and *Betula* spp., with juniper (*Juniperus communis*) and ericaceous
161 146 species (*Calluna*, *Empetrum*, *Vaccinium myrtillus*) making up the shrub layer. The herbaceous
162 147 layer includes monocotyledonous and dicotyledonous patches of anthropogenic origin (Aune,
163 148 1973). Although there is no stomach content data for these animals, the red deer population of
164 149 Åstfjorden, located in a similar environment 18 km away, consumes 55.5% graminoids, 29.9%
165 150 herbs, and 14.6% shrubs. In this area, snow cover prevents access to the herbaceous layer for 4
166 151 to 5 months a year (Myserud, 2000). Hemne red deer were hunted between September and
167 152 December 2014. Norwegian red deer belongs to the sub-species *Cervus elaphus atlanticus* and
168 153 differs genetically from the French and Spanish red deer populations (Zachos et al., 2016).

169 154 The French population from **Paimpont** (N = 28; 48.0723, -2.1640, Fig. 1, Table 1) originates from
170 155 a small remaining portion of the **Broceliande Forest**, covering an area of 1200 hectares. It
171 156 comprises dry moorland and deciduous woodland, under a temperate climate with oceanic
172 157 influences (MNHN Natura 2000, 2017). The Broceliande population has strong genetic affinities
173 158 with the Domaine National de Chambord (France) population, which has been regularly used as
174 159 a source population to replenish French deer populations (Dellicour et al., 2011; Klein, 1990).

175 160 The deer included in this study were hunted between September 2005 and January 2006. In the
176 161 20th century, red deer abundance drastically decreased in the Iberian Peninsula. They were only
177 162 found in the southwestern area, especially in Sierra Morena. Many deer that recolonised other
178 163 Spanish hunting areas in the 20th century came from these mountains (Arenzana et al., 1965).

179 164 **Alt Pallars** red deer (N = 16; 42.5452, 1.2789, Fig. 1, Table 1) come from a National Game
180 165 Reserve of Alt Pallars, a high mountain game reserve covering an area of 81,772 ha in the Spanish
181 166 Axial Pyrenees. Climate is Atlantic and subalpine, with wet and temperate summers and very

183 167 cold winters and spring with significant snow cover (Gort-Esteve et al., 2023; Pérez-González et
184 168 al., 2023). The sub-alpine belt is characterised by fir (*Abies alba*) and mountain pine (*Pinus*
185 169 *uncinate*). The montane belt is characterized by Scots pine (*P. sylvestris*) and extensive
186 170 deciduous forests composed of sessile oak (*Quercus petraea*), hazel (*Corylus avellana*), birch
187 171 (*Betula pendula*), aspen (*Populus tremula*) or ash (*Fraxinus excelsior*). The montane landscape
188 172 also includes rocky outcrops and Pyrenean broom (*Genista balansae*) and grasslands are
189 173 abundant. Human activity (managed meadows and a few agricultural fields) is significant in the
190 174 valley bottoms (Gort-Esteve et al., 2023). The red deer from Alt Pallars were hunted between
191 175 2015 and 2019, mainly during the hunting season between September and February. The
192 176 population of the National Game **Reserve of Boumort** (13,097 ha), located in the Pre-Pyrenees
193 177 (N = 18; 42.2313, 1.1235, Fig. 1, Table 1), is also located in the Spanish Pyrenees. Compared to
194 178 Alt Pallars, this region is characterized by lower mountains, and an overall milder climate with
195 179 hot and dry summers and cold winters with less snow accumulation. Most rainfall occurs in
196 180 spring and autumn (Gort-Esteve et al., 2023; Pérez-González et al., 2023). Subalpine grasslands
197 181 can be found, but the dominant vegetation consists of pine forests with an undergrowth of
198 182 bearberry (*Arctostaphylos uvaursi*) and juniper. Additionally, there are Scots pine and Pyrenean
199 183 pine (*P. nigra subsp. salzmannii*) forests. At lower elevations, there is a mixture of holm oaks (*Q.*
200 184 *ilex*) forest and extensive areas of thermophilic bushes. The red deer from Boumort were hunted
201 185 mainly between September and February, from 2013 to 2018. Alt Pallars red deer consume
202 186 49.1% of graminoids, whereas Boumort deer only consume 32.9% (Gort-Esteve et al., 2023). A
203 187 genetic study including these two Pyrenean red deer populations has recently been conducted
204 188 (Pérez-González et al., 2023). Despite being geographically close, they belong to genetically
205 189 different clusters: Alt Pallars deer show more genetic similarities with *Cervus elaphus* from the
206 190 south of France while the red deer of Boumort are genetically closer to the Iberian red deer
207 191 (*Cervus elaphus hispanicus*).

209 192 Deer sampled from Southern Spain come from the two independent mountains **Selladores-**
210 193 **Contadero** (N=31; 38.3497, -3.8428) and **Valquemado** (N=36; 38.2287, -4.1624, Fig. 1, Table 1),
211 194 both located in Sierra Morena Oriental, in the Natural Park of Sierra de Andújar, Jaén. The deer
212 195 studied from Valquemado were hunted in 1994-95 and the deer from Selladores-Contadero in
213 196 the 2018-2019 hunting season, from October to February. These areas are characterised by a
214 197 Mediterranean ecosystem with mild winters, precipitation in spring and autumn, very little
215 198 rainfall and high summer temperatures. In both localities, the Mediterranean pasture habitat
216 199 predominates is the Dehesa of holm oak and grassland vegetation, and some areas of
217 200 reforestation pine forests, and mastic trees (Marañón, 1991). In this area, the red deer annual
218 201 diet is mainly composed of herbaceous monocotyledons (57.1%; Azorit et al., 2012), with a peak
219 202 in spring. Browsers constitute an important food resource at the end of winter and of summer,
220 203 while fruits are consumed more in autumn and winter. In these regions, the genetic identity
221 204 corresponds to the Iberian deer subspecies (*Cervus elaphus hispanicus*).

222 205 El Durazno material is currently stored in the mastozoological collection of the Bioresearch
223 206 Center of the National University of the Northwest of the Province of Buenos Aires, Argentina.
224 207 Hemne and Paimpont specimens are stored at the Palévoprim lab (UMR6272, CNRS & University
225 208 of Poitiers, France). Alt Pallars, Boumort, Valquemado, and Selladores-Contadero specimens
226 209 belong to the Vertebrate Laboratory collection of RNM-175 Research Group, housed at the
227 210 University of Jaén, Spain.

228 211 **Rusa deer material**

229 212
230 213 The unique population of New Caledonian rusa deer (Frantz et al., 2024) lives in a wide range of
231 214 habitats, from man-managed plains to pristine dry forests, within various microclimates and
232 215 varying densities of herbivores (Fig. 1). There, its natural disaster status justifies almost
233 216 unlimited hunting 365 days a year. Between 2008 and 2022, a “jawbone reward” has been
234 217 introduced to encourage the local residents to shoot them. This study centres on animals
235 218 sampled throughout the year in 2018-2019 from four contrasting local New Caledonian habitats.

237 219 To date, there have been no studies of stomach content in these animals. The first sample comes
238 220 from a cattle-breeding area in the surroundings of the municipality of **Poya** (N=54, 165.1972, -
239 221 21.4605), on the west coast of New Caledonia, between Poya Bay and the Goulvain cape. In this
240 222 coastal region, the vegetation consists mainly of niaoulis savannah, composed of trees and
241 223 shrubs scattered throughout a dense herbaceous layer typical of the western coast of New
242 224 Caledonia, and agricultural grasslands. This area is particularly arid. The second habitat is the
243 225 **Grandes Fougères Provincial Park** (N=26, 165.7598, -21.6106), which straddles the
244 226 municipalities of Farino, Moindou, and Sarramea. This dense tropical rainforest, spanning 4,500
245 227 hectares, is home to many endemic vegetal and animal species. Deer have caused significant
246 228 damage in the area, especially to woody vegetation. However, deer pressure on the vegetation
247 229 has slightly decreased since the implementation of a more intensive hunting program. A third
248 230 group of animals (N=38) was hunted in the **Gouaro Déva Provincial Park** (Bourail; 165.3769, -
249 231 21.5735). This protected natural area of 7,800 hectares includes 1,700 hectares of sclerophyllous
250 232 forest, making it the largest dry forest area in New Caledonia. The park also has extensive
251 233 grasslands, niaoulis savannah and meso-sclerophyll formations. Since 2008, an intense and
252 234 effective daily hunting effort has significantly improved the vegetation growth in the park, which
253 235 was previously severely affected by the high deer density. The last sample consists of 12
254 236 specimens from a mountainous area called "**Vallée Misère**", located between Moindou and
255 237 Nessadiou. This forest, characterised by mesophyll vegetation, is seldom hunted due to access
256 238 challenges, which is only possible through private properties. Due to the very high density of
257 239 deer, the undergrowth of this forest is literally devastated, laid bare by the over-consumption
258 240 of the herbaceous layer and any regrowth of woody plants, as well as by trampling.

259 241 All rusa deer specimens included in this study are part of a larger collection of biological material
260 242 from New-Caledonian rusa deer belonging to the University of Poitiers (CVCU) and housed at
261 243 the Palévoprim laboratory (UMR7262, CNRS & University, Poitiers, France).

Methods

We applied 2D geometric morphometric method, a powerful and fully quantitative approach to capture interspecific, interpopulation, and intrapopulation shape variations (Hammer and Harper, 2008; Lawing and Polly, 2010; Zelditch et al., 2012). To do so, each specimen was positioned perfectly horizontally by placing it on its lingual surface on a support made of ground coffee, following the protocol described in Azorit et al. (2020).

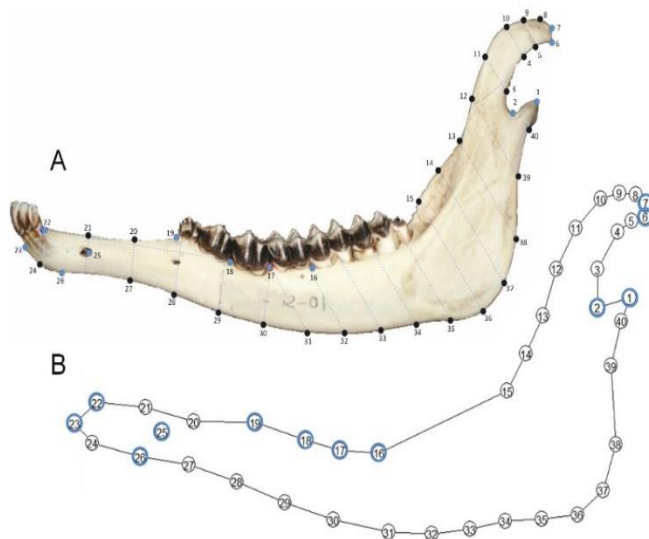


Figure 2: Landmarks (blue) and semi-landmarks (black) used to capture the mandibular bone morphology through a 2D geometric morphometric analysis on the buccal side of the left hemimandible. A: mandible of a red deer specimen from the Selladores-Contadero population showing the linear scheme by Makefan8 program to digitize the semilandmarks. B: Consensus shape for *Cervus elaphus*. The anatomical structures and regions corresponding to numbers 1-40 are described in Table 2.

All photos were taken with a Canon 7D digital camera, and a professional photographic table equipped with a graduated arm and lighting, allowing the camera to be perpendicular to the specimen. Each photo was taken at 50 cm distance with the same objective and settings, minimising image distortion and parallax error. We focused on the left hemimandible, but when unsuitable, we photographed the right hemimandibles and flipped it horizontally to obtain the jaw buccal surface. Adapting the existing protocol developed for similar mandibular studies (Azorit et al., 2020), we digitized 40 landmarks and semilandmarks on the mandible to capture

its shape using TPSDig2 (Rohlf, 2021). Since the homology is provided by the geometry of the mandibular structures or by biological characteristics, unique and easy to identify in all the individuals studied, the reference points 1, 2, 6, 7 and the group of 16-19, 22, 23, 25 and 26 are considered type II and I landmarks, respectively (Fig. 2, Table 2). To obtain a description of the mandibular curved edges, we used the Makefan8 tool of the Integrated Morphometric Software 8 Package (IMP 8) (Sheets, 2014). It is a graphical tool for selecting points to digitize semilandmarks along a curve and it is based on the creation of a scheme of equidistant lines between two landmarks. Figure 2 shows the linear reference scheme created to digitize the semilandmarks along the curves in a standardized manner across all specimens. Then, the semilandmarks were slid, to the position minimizing the squared Procrustes distance between the form of the hemimandible of a given specimen and the consensus reference form from all specimens, using gmShiny (v. 0.1.4) (Baken et al., 2021; Zelditch et al., 2012).

Table 2: Description of landmarks and semilandmarks used for capturing the mandibular shape for geometric morphometric analyses.

| Landmarks | Names and Description |
|---------------|--|
| 1 | Tip of the condylar process |
| 2 | Ventral margin of the mandibular sigmoid notch |
| 6 | Ventrocaudal margin of the coronoid process |
| 7 | Tip of the coronoid process |
| 16 | Posterior alveolar margin of <i>M1</i> |
| 17 | Anterior alveolar margin of <i>M1</i> |
| 18 | Posterior alveolar margin of <i>P3</i> |
| 19 | Anterior alveolar margin of <i>P2</i> |
| 22 | Posterior alveolar margin of <i>C</i> |
| 23 | Ventral margin of the <i>I1</i> |
| 25 | Mental foramen |
| 26 | Posterior margin of the mandibular symphysis |
| Semilandmarks | Description traits |
| 3 to 5 | Concavity of the posterior border of the coronoid apophysis |
| 8 to 15 | Convexity of the anterior edge of the coronoid process |
| 20 to 21 | In the mandibular diastema, at the level of the Semilandmark 27 (20) and of the Landmark 25 (21) |
| 24 | Rostro-ventral margin of the horizontal ramus of the mandible, at the level of the posterior alveolar margin of <i>C</i> |
| 27 to 38 | Convexity of the ventral margin of the horizontal ramus of the mandible to the posterior margin of the angular process |
| 38 to 40 | Concavity of the caudal edge of the mandible ramus |

Geometric morphometric analyses were performed with the R package Geomorph v. 4.0 (Adams et al., 2024; Baken et al., 2021). We obtained the centroid size (i. e. the square root of the sum of the squared distances of a set of landmarks from their centroid) for each specimen.

Statistical analyses

We first explored the differences in centroid size between groups using analyses of variance (ANOVAs) for each of the three datasets (for *Cervus elaphus* plus *Rusa timorensis*; for all *Cervus elaphus*; and for all *Rusa timorensis*; Annex 1), followed by Duncan's post-hoc tests where appropriate. We also did a generalized Procrustes analysis on the raw landmark coordinates for all specimens of each of the three datasets to remove differences in size, translation, and rotation. We then explored the structure of the variance using a Principal Component Analysis (PCA) on each of these datasets. The ANOVAs on the PC scores representing more than 80% of the variance were performed to detect between-group (species; populations; habitats)

315 284 differences. Where differences were detected, post hoc Duncan's tests were conducted to
316 285 identify between which groups these differences were located. For axes showing significant
317 286 differences, we describe the morphological variations along each PCA axis.

318 287 Then, with Canonical Variate Analyses (CVA) maximising the between-group differences, we
319 288 focused on the morphological variations enabling us to differentiate between populations
320 289 (dataset *Cervus elaphus*) and habitats (dataset *Rusa timorensis*). We also performed ANOVAs on
321 290 canonical variates, followed by Duncan post-hoc tests where appropriate. We describe the
322 291 morphological differences along each axis where significant differences exist between groups.
323 292 Together, PCA and CVA provide a comprehensive understanding of the data structure and group
324 293 differences. Finally, for the *C. elaphus* populations for which these data were available, we
325 294 looked at the correlation between mandible shape variations and two explanatory variables: the
326 295 percentage of herbaceous monocotyledons consumed annually and the latitude.

327 296 Procrustes regressions and Partial Least Square (PLS) analyses enabled us to investigate the
328 297 relative influence of the animals' size (allometry/isometry) and population (for *Cervus elaphus*)
329 298 or habitat (for *Rusa timorensis*) on the mandibular morphology of the deer.

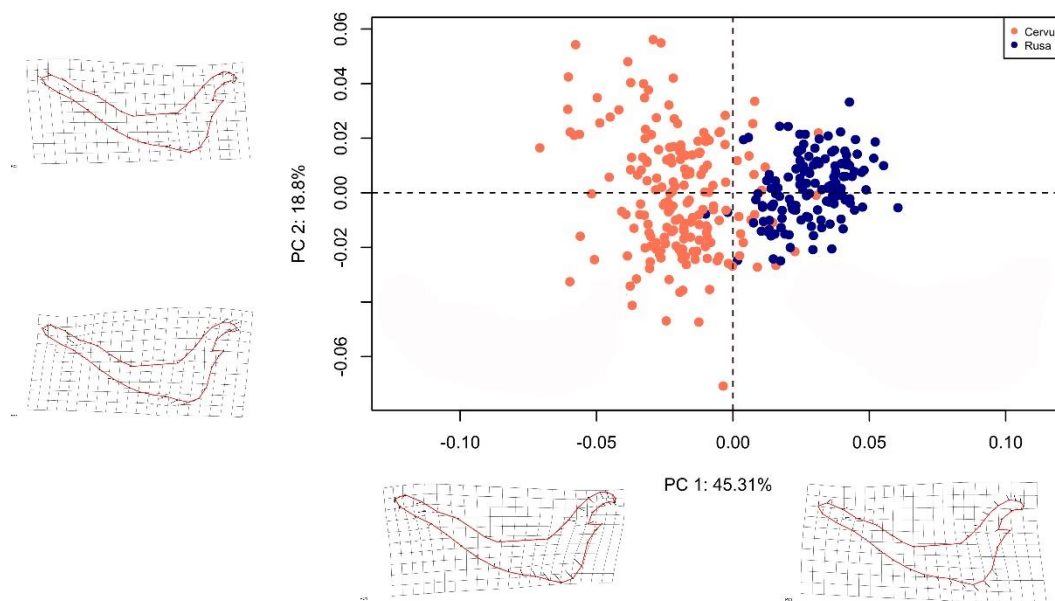
330 299 **Results**

331 300 **Interspecific differences:**

332 301 There is a significant difference of centroid size between the two species ($p < 2.2e-16$; Table S1,
333 302 Annex 1), with *Cervus elaphus* being significantly larger. The first four principal components
334 303 (PC1-4) of the PCA represent over 80% of the variance (Annex 1). ANOVAs on the PC scores show
335 304 that species statistically differ on PC1 ($p < 2e-16$; Table S1), PC3 ($p = 7.12e-15$; Table S1) and PC4
336 305 ($p = 0.0141$; Table S1).

337 306 *Cervus elaphus* occupies the lower values on PC1 (45.3%; Fig. 3), with thinner and more slender
338 307 mandibles compared to *Rusa timorensis*, which has higher values on PC1. The angle made by the
339 308 ramus and the corpus on the internal side of the mandible is more perpendicular in *Rusa*

341 309 *timorensis* and more open in *Cervus elaphus*. The angular process (anatomical region 34 to 39 in
 342 310 Fig. 2) of *Rusa timorensis* is more voluminous, rounded and robust. Its coronoid process is
 343 311 thicker, less elongated posteriorly and less pointy. The posterior margin of the mandibular
 344 312 symphysis is more concave in *Cervus elaphus*, and straighter and oriented upwards in *Rusa*
 345 313 *timorensis*. On PC3 (10.2%; Annex 1), *Cervus elaphus* occupies the higher values. Shape
 346 314 deformation reflects a more pronounced concavity in the anterior margin of the mandibular



347 Figure 3: Biplot representing the two first principal components of the PCA exploring interspecific mandibular shape
 348 variations between *Cervus elaphus* and *Rusa timorensis*. Shape deformations are shown along PC1 and 2 for each species
 349 (*C. elaphus*: coral; *R. timorensis*: navy blue). The consensus shape for all Cervini is shown in grey to aid interpretation.

350 315 angle, at the level of the vascular incisure, for *Cervus elaphus* compared to *Rusa timorensis*. On
 351 316 PC4 (5.8%; Annex 1), interspecific differences are less obvious and seem to be due to a few
 352 317 outlying individuals.

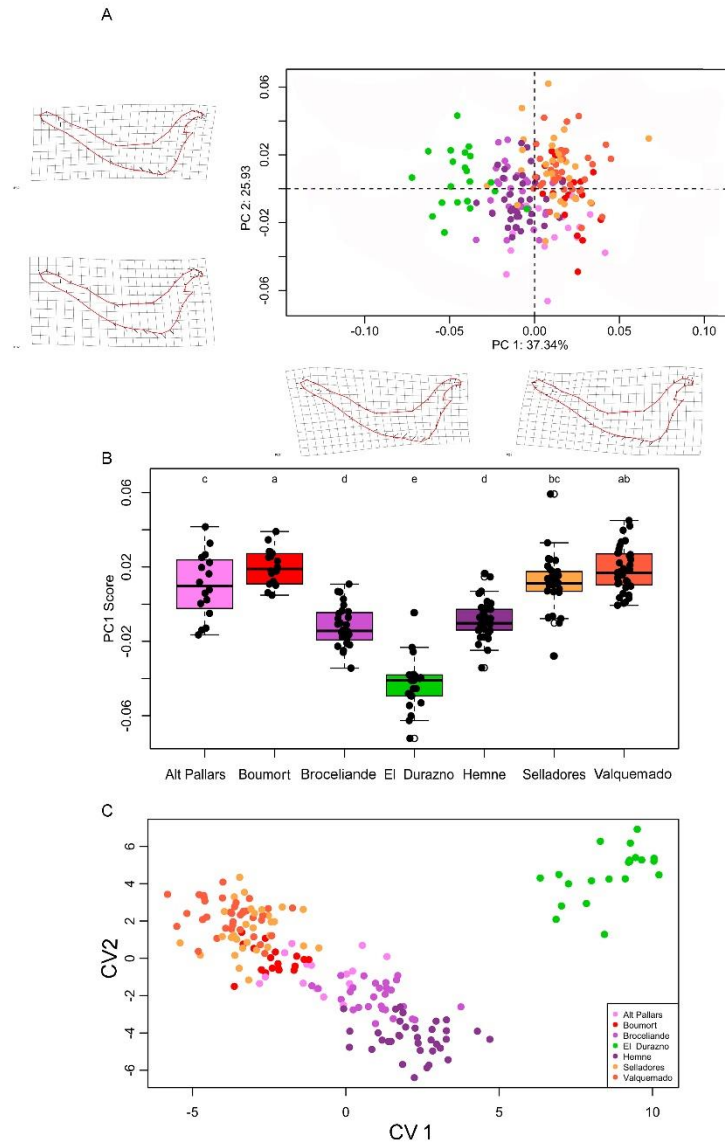
353 318 **Interpopulation differences: between *Cervus elaphus* populations**

354 319 There are significant differences in centroid size ($p < 2.2e-16$; Table S1) among the seven *Cervus*
 355 320 *elaphus* populations considered. Based on Duncan's post-hoc tests (Table S2; Annex 1), the El
 356 321 Durazno deer is significantly larger than the European populations, whereas Boumort deer

358 322 constitute the smaller population. The second smallest *Cervus elaphus* are those of Valquemado
359 323 population. It significantly differs from the larger deer found in Alt Pallars and Broceliande.
360 324 Hemne and Selladores-Contadero fall between Valquemado and the group of Alt Pallars and
361 325 Broceliande, and do not statistically differ in size from either of them.

362 326 PC1-5 of the PCA exploring the shape deformation among these populations represent more
363 327 than 80% of the variance (Annex 1). ANOVAs on PC scores indicate significant differences
364 328 between populations on each of these PC ($p < 0.05$ in all cases; Table S1). Interpopulation
365 329 differences are identified based on Duncan's post-hoc tests (Table S2). On PC1 (percentage of
366 330 explained variation: 37.3%; Fig. 4, A and B), the El Durazno population of *Cervus elaphus* stands
367 331 out as having the most negative values. The Boumort population has the highest values and is
368 332 statistically different (Fig. 4 B; Table S1 and S2) from all the other populations. Alt Pallars, Hemne
369 333 and Broceliande populations differ significantly from the first two, with high to medium values
370 334 on PC1. Finally, Selladores-Contadero and Valquemado are similar to each other, with high
371 335 values on PC1, and do not differ significantly from Alt Pallars and Boumort, respectively (Table
372 336 S2; Annex 1). Morphologically, specimens in the low PC1 range have a more elongated diastema
373 337 than populations with higher values. These specimens also have a lower vertical ramus and a
374 338 less pronounced mandibular sigmoid notch. Their corpus is straighter and less convex in its
375 339 ventral margin. The posterior margin of the mandibular symphysis is more concave in these

377 340 individuals with low PC1 values. Alt Pallars deer occupy the lower values of PC2 (25.9%; Fig. 4 A;
 378 341 Table S2; Annex 1), statistically differing from Selladores-Contadero and Valquemado, which are
 379 342 in the higher range. Hemne falls between these two extremes and is statistically different from



380
 381
 382
 383
 384
 385
 386

Figure 4: A: Biplot representing the two first principal components of the PCA (63.3% of the variance) exploring Cervus elaphus interpopulation mandibular shape variations. Shape deformations are shown along PC1 and 2 for each population (Alt Pallars: pink; Boumort: red; Broceliande: mauve; El Durazno: green; Hemne: purple; Selladores: dark yellow; Valquemado: orange). The consensus shape for all C. elaphus is in grey to aid interpretation. B: Focus on the variation on PC1. Letters (a-e) represent interpopulation differences based on Duncan post hoc test. C: Biplot representing the two first canonical variates of the CVA.

387

388 343 both. Boumort, Broceliande and El Durazno populations have values between Hemne and the
389 344 two populations of Southern Spain, with El Durazno being closer to the populations in Southern
390 345 Spain and Boumort and Broceliande being closer to Hemne. These statistical differences are
391 346 reflected in deformations along PC2 (Fig. 4 A; Annex 1). In individuals with negative values of
392 347 PC2, the ramus and corpus of the mandible appear more robust, with a more pronounced and
393 348 rounder angular process. The angle between the ramus and the corpus of the mandible is
394 349 perpendicular for specimens with lower PC2 values and becomes more obtuse in those with
395 350 higher values. Additionally, in specimens with lower PC2 values, the ramus of the mandible is
396 351 higher, and the corpus of the mandible is more elongated and directed upward.

397 352 The Duncan test reflects fewer differences on PC3 (Annex 1). The Selladores-Contadero
398 353 population, with higher values, significantly differs from the populations of El Durazno and
399 354 Boumort, both characterized by lower values. With intermediate values on PC3, the four other
400 355 populations are not significantly different from Selladores, El Durazno and Boumort.

401 356 There is a moderate correlation between the shape of the mandible on PC1 and the latitude
402 357 (Annex 1: correlation of -0.56 between these two variables, see also the graphic "Correlation
403 358 between Latitude and PC1"), whereas the correlation is weak between the percentage of
404 359 graminoids and the latitude (Annex 1: correlation = -0.21, see also the graphic "Correlation
405 360 between %_{graze} and PC1").

406 361 ANOVAs performed on the six canonical variables of the Canonical Variate Analysis (CVA) all
407 362 support significant differences ($p < 2e-16$ for CV1-6; Table S1, Annex 1), further identified via
408 363 Duncan's post-hoc tests (Table S2). On CV1 (Fig. 4 C), all populations differ statistically. The
409 364 European populations show a range of low to medium values on CV1, while the Argentina
410 365 population of El Durazno exhibit the highest value. More specifically, the populations of
411 366 Selladores-Contadero and Valquemado (Southern Spain) have the lowest values, followed by
412 367 the Alt Pallars and Boumort populations (Northern Spain). The French population of Broceliande
413 368 and the Norwegian population of Hemne have medium values. The shape deformations on CV1

415 369 mainly concern the length of the corpus of the mandible, the length of its ramus and the shape
416 370 of the vascular incisure, at the anterior margin of the angular process. Specimens in the low CV1
417 371 range are characterised by a shorter corpus and a higher ramus than specimens in the high CV1
418 372 range. The vascular incisure is clearly convex in *Cervus elaphus* individuals in the low values of
419 373 CV1, whereas it is concave in specimens with higher values. All populations differ statistically on
420 374 CV2 (Fig. 4 C; Tables S1 and S2; Annex 1). The Norwegian population of Hemne is situated in the
421 375 lower range, followed by Broceliande, Alt Pallars, and Boumort. Selladores-Contadero and
422 376 Valquemado have intermediate values, while El Durazno occupies the higher range of CV2.
423 377 Morphological deformations on CV2 are located on the coronoid process, higher and less
424 378 posteriorly oriented for specimens with lower values. For these individuals, the angular process
425 379 is also more robust, and the posterior margin of the mandibular symphysis is less concave.
426 380 A correlation of 0.85 suggests a strong linear relationship between latitude and CV1 (Annex 1,
427 381 see also the graphic “Correlation between Latitude and CV1”), whereas a correlation of 0.02 (see
428 382 also the graphic “Correlation between %graze and CV1” in Annex 1) means there is no relation
429 383 between the latitude and the percentage of herbaceous monocotyledons.

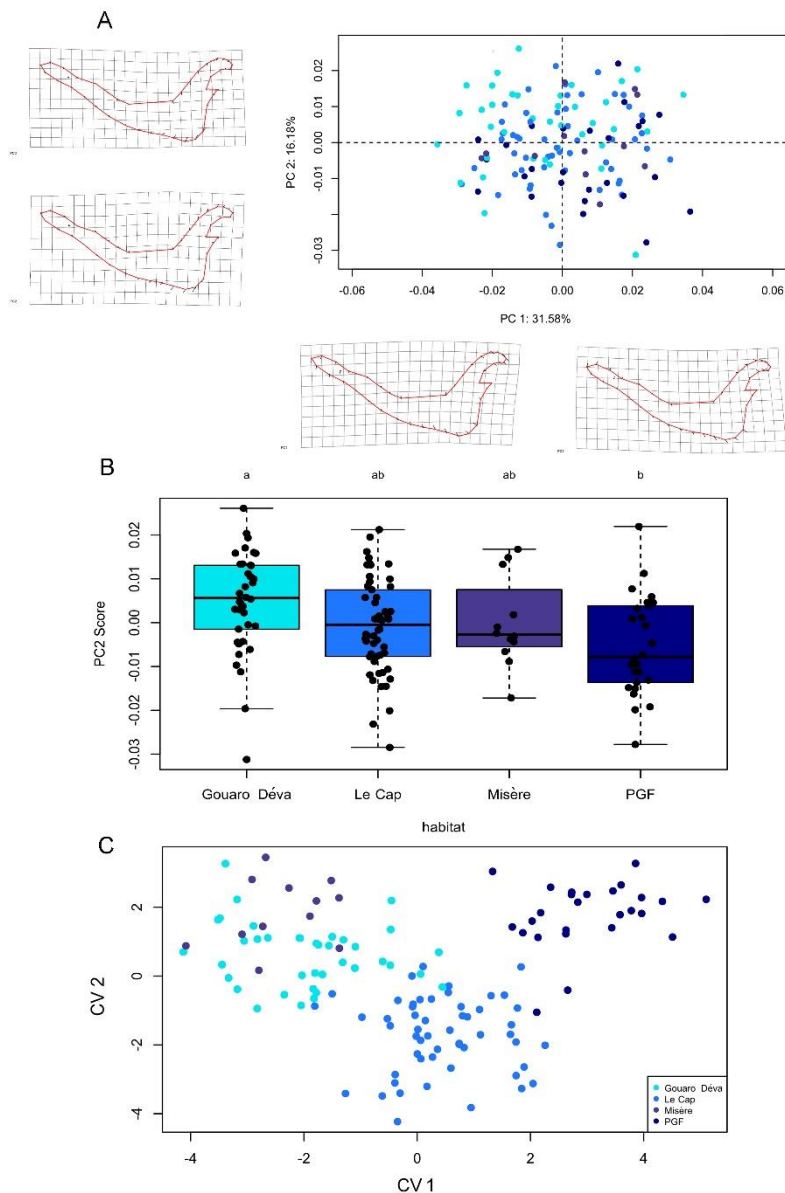
430 384 **Inter-habitat and intrapopulation differences: *Rusa timorensis* from contrasting**
431 385 **habitats**

432 386 Based on the analysis of variance (ANOVA), the centroid size of *Rusa timorensis* specimens from
433 387 the various contrasting habitats differs significantly ($p = 9.61e-05$; Table S1). According to
434 388 Duncan's post-hoc test, *Rusa timorensis* from Gouaro Déva are significantly smaller than rusa
435 389 deer from the other three habitats (Table S2; Annex 1).

436 390 PC1-8 of the PCA represent over 80% of the variance. Only PC2, 5 and 6 show significant
437 391 differences between the four habitats (p -values < 0.05 in all cases; Table S1, Annex 1). Based on
438 392 the Duncan post hoc test (Table S2), we can statistically differentiate between the Gouaro Déva
439 393 animals, which exhibit the highest values on PC2 (16.2% of the explained variance, Fig. 5 A and
440 394 B), and the deer from the Parc des Grandes Fougères, which show the lowest values. Deer from

442 395 Le Cap and Misère are not statistically different from the others. Morphologically, these
443 396 differences are found in the condylar process, which goes further back in animals with high PC2
444 397 values, and in the mandibular symphysis, which is more upward-oriented in these same

446 398 individuals. In these animals, the angular process is more robust, whereas it is frailer and
447 399 concave at the level of vascular incisure in animals with low values on PC2.



448 *Figure 5: A: Biplot representing the two first principal components of the PCA (47.76% of the*
449 *variance) exploring *Rusa timorensis* intrapopulation mandibular shape variations between*
450 *contrasting habitats. Shape deformations are shown along PC1 and PC2 (Gouaro Déva:*
451 *Turquoise, Le Cap: royal blue, Misère: plum, Parc des Grandes Fougères (PGF): navy blue).*
452 *The consensus shape for all *R. timorensis* is in grey to aid interpretation. B: Focus on the*
453 *variation on PC2. Letters a and b represent interpopulation differences based on Duncan's*
454 *post hoc test. C: Biplot representing the two first canonical variates of the CVA.*

455 400

456

457 401 The fifth principal component represents 5.7% of the variance (Annex 1). Deer from the Parc des
458 402 Grandes Fougères stand out with high PC5 values, which are statistically different from the low
459 403 values of Gouaro Déva and Misère deer on this axis. Deer from Le Cap present intermediate
460 404 values and are not different from the other deer. On PC5, specimens with low values have a
461 405 well-rounded angular process, unlike specimens with high values, whose angular process
462 406 protrudes backwards. The rest of the mandible is fairly stable along PC5.

463 407 On PC6 (4.4% of the variance; Annex 1), a significant statistical difference exists between the
464 408 higher values of Gouaro Déva deer and the lower values of Parc des Grandes Fougères deer. Le
465 409 Cap and Misère deer show intermediate values and are not statistically different from the first
466 410 two groups. The morphological differences on PC6 are mainly situated in the posterior margin
467 411 of the ramus of the mandible, which is more robust in animals with low PC6 values. The
468 412 mandibular symphysis of these specimens is also straighter. On specimens with higher values it
469 413 is turned slightly downwards.

470 414 ANOVAs on the three canonical variables of the Canonical Variate Analysis (CVA; Table S1, Annex
471 415 1) all support significant differences ($p < 2e-16$ for CV1-3). Gouaro Déva and Misère deer
472 416 constitute one group with lower values of CV1 (Fig. 5 C; Annex 1), which is statistically different
473 417 from Parc des Grandes Fougères deer situated in the higher values of this axis and from Le Cap
474 418 with intermediates values. The coronoid process of individuals in the high CV1 range is more
475 419 voluminous. The concavity of the vascular incisure is more pronounced in the lower values of
476 420 CV1. In addition, the mandibular symphysis of these animals is oriented more upwards than in
477 421 animals with high values on this axis.

478 422 On CV2 (Fig. 5 C; Annex 1), we statistically distinguish Le Cap, with low values, from a group
479 423 gathering together Parc des Grandes Fougères and Misère, and from Gouaro Déva deer (Table
480 424 S2). The last three populations present positive values on CV2. The mandibular symphysis is
481 425 more oriented downwards for individuals with high CV2 values. The vascular incisure of these

483 426 animals is slightly more concave, and the coronoid process is slightly lower and projected further
484 427 back.

485 428 Finally, we identify three statistically different groups along CV3. Misère deer are characterized
486 429 by high values, Le Cap and Parc des Grandes Fougères deer by medium values, and Gouaro Déva
487 430 deer by lower values. Shape variations along this axis are subtle. The ramus of the mandible
488 431 appears to be slightly less robust at its anterior margin in animals with low values. The condylar
489 432 process is projected slightly further back in the same animals.

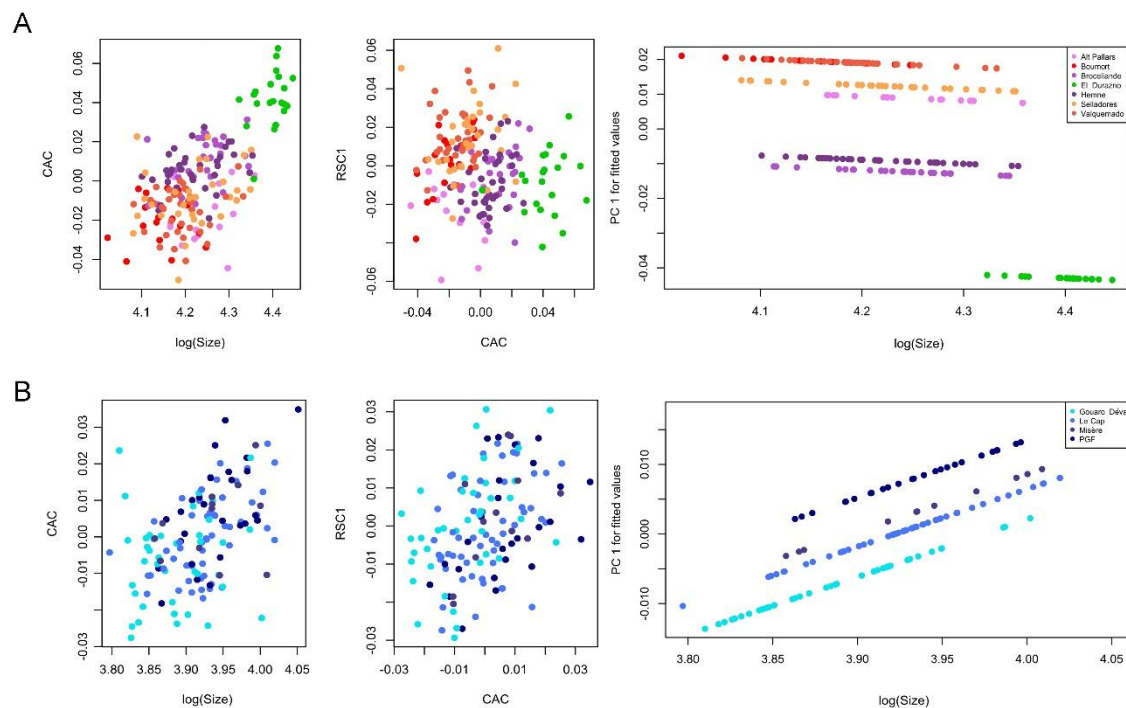
490 433 **Allometry**

491 434 The Procrustes regression (Procrustes distance-based linear model) performed on the first
492 435 dataset "*Cervus elaphus* plus *Rusa timorensis*" indicates that both "centroid size" and "species"
493 436 significantly explain shape differences between species (p-values =0.001; Table S3; Annex 1). R^2
494 437 indicate that 33.7% of the variance in this dataset is explained by log (Centroid size), and 5.6%
495 438 by the species (Table S3). But these two variables are not independent (Annex 1: $r_{pb} = -0.878$).
496 439 Within each population, there is a quasi-isometry (Fig. 6).

497 440 Regarding *Cervus elaphus* there is a moderate-strong (r-PLS: 0.641; Table S5) and statistically
498 441 significant (p-value= 0.001; Table S5) correlation between centroid size and mandible shape. The
499 442 variance explained by size is $R^2 \approx (r\text{-PLS})^2 = 0.428$, indicating that 43% of the variation in shape is
500 443 due to size, while 57% is explained by other factors (Annex 1). Centroid size explains only half as
501 444 much of the between-group differences as the population does ($R^2_{\text{population}} = 0.29$; $R^2_{\text{centroid size}} =$
502 445 0.14; Table S3). For PC1-5, where shape differences were observed between populations, the
503 446 same observation was made: it is the population that explains most of the variance in the model
504 447 ($R^2_{\text{Population}} > R^2_{\text{Centroid size}}$ in most cases; Table S4; Annex 1). Moreover, the allometry plot (Fig. 6 A;
505 448 Annex 1) suggests a quasi-isometry, with the shape of *Cervus elaphus* mandibles not varying
506 449 significantly when size increases inside each population. Finally, the Partial Least Squares
507 450 analysis (Table S5), which aims to maximise the covariance between centroid size and

509 451 mandibular shape, estimates that the correlation between the centroid size and the mandibular
 510 452 shape is statistically significant ($p = 0.001$) and moderate to strong ($r\text{-PLS} = 0.641$).

511 453 For *Rusa timorensis*, the variance explained by size is $R^2 \approx (r\text{-PLS})^2 = 0.216$, indicating that only 22%
 512 454 of the variation in shape is due to size, while 78% is explained by other factors (Fig. 6 B, Annex
 513 455 1), such as the habitat to which the individuals belong ($p = 0.030$; Table S3). Based on R^2 , 4.4%
 514 456 of the variance is explained by log (centroid size) and 3.7% by the habitat (Table S3). The



515 *Figure 6: Allometric relationships and morphological variation in Cervus elaphus from different populations (A) and Rusa*
 516 *timorensis from contrasted local habitats (B). Plots illustrate body size and shape variations, both within and among*
 517 *Cervini populations, highlighting population-specific morphological trends. Log (Size): log-transformed body size; CAC and*
 518 *RSC1 are morphological metrics. CAC: Common Allometric Component; RSC1: Residual Shape Component 1; PC1:*
 519 *Principal Component 1. The rightmost plots provide information regarding allometry or isometry.*

520 457 procrustes regressions performed on each axis of the PCA identifying morphological differences
 521 458 between habitats (PC2, PC5, PC6) show that on PC2 and PC6, only centroid size influences
 522 459 variations in mandible shape (p -values of 0.004 and 0.002 respectively; R^2 of 0.07 and 0.09
 523 460 respectively; Table S4, Annex 1). On PC5, on the other hand, only the habitat is responsible for
 524 461 the morphological variations ($p = 0.002$; $R^2 = 0.13$; Table S4, Annex 1). Finally, the Partial Least
 525 462 Squares analysis estimates that the mandibular bone morphology of *Rusa timorensis* shows a

527 463 moderate (r -PLS= 0.465; less than for *Cervus*; Table S5) and statistically significant ($p = 0.001$;
528 464 Table S5) correlation between centroid size and mandible shape.

529 465 **Discussion**

530 466 **Interspecific differences**

531 467 Shape differences between the two species reflect distinct evolutionary histories (Mackiewicz
532 468 et al., 2022; Raia et al., 2010). These differences can be related to different biomechanical needs
533 469 associated with contrasting feeding ecologies for the two species (Clauss et al., 2008). Indeed,
534 470 *Cervus elaphus*, a generalist ungulate that can adjust its diet from grazing to browsing (Azorit et
535 471 al., 2012; Bugalho and Milne, 2003; Gębczyńska, 1980) depending on the availability of resources
536 472 in its habitat (Gebert and Verheyden-Tixier, 2001), has a mandible that is generally more slender
537 473 and thinner than that of *Rusa timorensis*. The angle made by the ramus and the corpus on the
538 474 internal side of the mandible is obtuse. The angular process has a concave shape at the level of
539 475 the vascular incisure. In contrast, *Rusa timorensis* from New Caledonia is highly selective
540 476 towards herbaceous monocotyledons (Berlioz et al., 2020). The architecture of its mandible is
541 477 more orthogonal and straighter with a robust angular process corresponding to the insertion
542 478 zone of the Masseter and Pterygoid muscles (Greaves, 1991; Kangas et al., 2017; Pérez-Barbería
543 479 and Gordon, 1999). Compared to the red deer mandibles, rusa deer mandibles are better shaped
544 480 to withstand the larger biomechanical stress and mastication forces expected from a grazer diet
545 481 (Kangas et al., 2017; Raia et al., 2010).

546 482 **Differences between *Cervus elaphus* populations**

547 483 Results showed that the shape variations among red deer are mainly explained by population
548 484 identity, and to a lesser extent by the size of the mandibles. The quasi-isometry observed and
549 485 the relative effect of size and population identity on the distribution (Fig. 6; Table S3), means
550 486 that intrapopulation variations in size have little impact on the morphological variations
551 487 observed. For this reason, the rest of the discussion focuses on interpopulation differences.

553 488 The significant size differences between the seven populations of red deer demonstrate the
554 489 polymorphic nature of this species (with sizes ranging from 50 kg to 400 kg; Geist, 1998). In
555 490 Europe, there is a significant size gradient between the morphologically largest populations in
556 491 Eastern Europe and the smallest in Southern and Western Europe (Lister, 1996). This is often
557 492 referred to as the Bergmann's rule, which states that larger size provides an advantage under
558 493 cold climates by reducing thermal loss. Such a trend is also observed at smaller scales, like among
559 494 Norwegian red deer populations (Langvatn and Albon, 1986). It is now more often associated
560 495 with the latitudinal clines in the primary productivity and the quality of the plants eaten by the
561 496 animals. This is because the water, light, and temperature conditions at higher latitudes favour
562 497 the growth of plants that are more nutritious (richer in proteins and soluble carbohydrates) and
563 498 more digestible due to their less lignified cell walls (Deinum, 1981; Langvatn and Albon, 1986
564 499 and references therein). These characteristics strongly influence animal growth and weight gain
565 500 (Langvatn and Albon, 1986; McNab, 2010: also referred as the "Resource rule"). However,
566 501 among the seven red deer populations studied here, we observed no size cline correlated with
567 502 latitude (Table S3; Annex 1). The study of a larger number of populations along this latitudinal
568 503 range would probably make it possible to reduce the influence of habitat-specific characteristics
569 504 (i.e., distance from the coast, topography, altitude, etc.) and thus highlight such a trend.

570 505 El Durazno population, which comes from the Eastern European genetic lineage of *Cervus*
571 506 *elaphus*, is characterised by larger body sizes. We also found that the largest individuals in our
572 507 study came from this population. Individuals sampled from populations genetically closer to the
573 508 Iberian red deer *C. elaphus hispanicus* (Selladores, Valquemado and Boumort) were located at
574 509 the lower end of the body size continuum. If poor environmental conditions can explain overall
575 510 interpopulation differences in body size (Azorit et al., 2020), we cannot completely rule out the
576 511 role of genetics in size variation.

578 512 Numerous studies have highlighted the strong association between the shape of the mandible,
579 513 its biomechanical performances and the physical properties of the diet (Clauss et al., 2008;
580 514 Fletcher et al., 2010; Pérez-Barbería and Gordon, 1999; Raia et al., 2010; Spencer, 1995; Varela
581 515 and Fariña, 2015; Wang et al., 2022; Zhou et al., 2019). Here, there is a noticeable morphological
582 516 gradient in European red deer mandibles along a north-south transect from Southern Spain to
583 517 Norway, visible both on PC1 and CV1 (Annex 1). The vertical branch and the coronoid process of
584 518 the southernmost specimens are higher, which increases the biting force of the temporalis
585 519 muscle (Kangas et al., 2017; Pérez-Barbería and Gordon, 1999). The angle made by the ramus
586 520 and the corpus of the mandible is more acute and the angular process more developed on its
587 521 anterior margin, providing a greater insertion area for masticatory muscles such as the masseter
588 522 and pterygoid (Greaves, 1991; Pérez-Barbería and Gordon, 1999). Overall, the mandible of the
589 523 southernmost specimens is more robust, allowing for more efficient chewing of hard and tough
590 524 foods (Clauss et al., 2008). To the north, at the other end of the range, the mandibles are more
591 525 slender and gracile, indicating that less biting force is needed for mastication of the dominant
592 526 diet (Fletcher et al., 2010). Kangas et al. (2017) demonstrated a similar mandibular
593 527 morphological shift along a shorter North-South transect for moose populations in Finland under
594 528 a boreal climate. These authors associate a less robust mandible for northern moose with a
595 529 lower percentage of grasses in their diet. In our case, on a broader geographical scale, there is
596 530 no linear correlation between the percentage of herbaceous monocotyledons consumed and
597 531 the latitude (Annex 1), meaning that the percentage of herbaceous monocotyledons alone
598 532 (ranging from 30 to 60% for the populations in this study) is not a sufficient indicator to explain
599 533 this latitudinal gradient. The picture is indeed much more complex. The transect from Norway
600 534 to Southern Spain crosses many climatic regions (Dinerstein et al., 2017; Peel et al., 2007) and
601 535 vegetation units (Ozenda and Borel, 2000). As a result, the taxonomic composition of deer diets
602 536 varies greatly between populations. In addition, the percentage of graminoids doesn't reflect
603 537 the overall dietary composition of the animals. Furthermore, annual percentages of bushes and

605 538 trees, graminoids, forbs and fruits in the diet do not reflect the important seasonal dietary
606 539 variations (Azorit et al., 2012; Gort-Esteve et al., 2023; Mysterud, 2000; Pordomingo and Rucci,
607 540 2000). These seasonal dietary changes result both from the physiological needs of the animals,
608 541 notably in terms of nutrients (Verheyden-Tixier et al., 2008), and from behaviours aimed at
609 542 compensating for restrictions on access to certain resources (linked for example to the snow
610 543 cover : Albon and Langvatn, 1992; to plant phenology : Azorit et al., 2012; or to the seasonal
611 544 senescence of certain resources : Bugalho and Milne, 2003). Although not the most important
612 545 part of the diet, fallback food, which is important when preferred resources are unavailable, is
613 546 essential at certain times of the year. This is the case, for example, with acorns, which are eaten
614 547 by males in large quantities in autumn in Southern Spain (Azorit et al., 2012; Berlioz et al., 2017).
615 548 Such food items may require specific chewing forces to process and, therefore, the development
616 549 of masticatory muscles. The stems and leaves of some shrubs can be as tough or tougher than
617 550 some herbaceous monocotyledons (Berlioz, 2017; Merceron et al., 2010). Finally, for the same
618 551 type of food, the quality and physical composition can vary greatly depending on the season and
619 552 along a North-South transect (Hebblewhite et al., 2008). Different parts of the plant and plants
620 553 of different ages also have different physical properties. The example of herbaceous
621 554 monocotyledons provides a good illustration of this last point. In Southern Europe, summer is a
622 555 particularly difficult season for ungulates, as severe summer droughts lead to senescence of the
623 556 herbaceous layer, resulting in scarce food resources, of poor quality, fibrous and abrasive. This
624 557 resource type requires more force to process. In Northern Europe, on the other hand, while the
625 558 herbaceous layer is inaccessible to ungulates for several months of the year because of the snow
626 559 cover (Albon and Langvatn, 1992), when the snow melts, the animals have access to tender
627 560 young shoots, rich in protein and low in fibre (Hebblewhite et al., 2008; Langvatn and Hanley,
628 561 1993), requiring less chewing force. There, herbaceous monocotyledons do not reach fibre
629 562 compositions as high as those observed in summer in Southern Europe.

631 563 Geographical differences in the physical properties of dietary boluses inevitably affects the
632 564 chewing forces required for comminution. This will consequently affect the development of
633 565 masticatory muscles and mandibular bone morphology. Although we lack direct measures of
634 566 the physical properties of the diet, we expect that such factors can be partly responsible for
635 567 observed the north-south variation in mandibular morphology. To confirm this hypothesis,
636 568 changes in the physical properties of vegetation resources along a gradient between Norway
637 569 and Southern Spain would need further investigation.

638 570 The Argentinean red deer population from El Durazno is considered separately here as it displays
639 571 a unique morphology, with a finer mandibular angle and an even more pronounced slender
640 572 global morphology, that sets it apart from European populations. At El Durazno, the deer have
641 573 access to a savanna-like herbaceous layer, except in winter when the grass is dry. In winter,
642 574 these deer mainly feed on fruits and the leaves of trees and bushes (Pordomingo and Rucci,
643 575 2000). Both genetics and environmental factors could explain the peculiar aspect of the
644 576 mandibles of El Durazno deer. To go further and settle this question, exploring the variations in
645 577 mandibular shape between several populations of Argentinian red deer and representatives of
646 578 the original gene pool in Central Europe would be interesting.

647 579 **Inter-habitat differences: among *Rusa timorensis* population**

648 580 Together, body size and habitat account for around 8% of the shape variation observed in *Rusa*
649 581 *timorensis*. This low percentage is most likely explained by the recent introduction of a limited
650 582 number of individuals of the species to New Caledonia (Barrau and Devambe, 1957), but
651 583 nevertheless reflects a biological reality.

652 584 At first sight, the comparison of centroid sizes in rusa deer from contrasting habitats yields
653 585 results that are surprising. Indeed, the rusa deer of the Gouaro Deva Provincial Park, although
654 586 occupying a habitat rich all year round in herbaceous monocotyledons, the preferred resource
655 587 of these animals, are characterised by smaller body sizes than the other rusa deer in this study.

657 588 Body size differences between ungulate populations from different habitats can be related to
658 589 the availability, accessibility, and nutritional quality of resources, particularly during animal
659 590 growth (Azorit et al., 2020; Terada et al., 2012; Toïgo et al., 2006). This can be complicated when
660 591 access to resources is made difficult, such as in situations of interspecific or intrapopulation
661 592 competition when animal density is high (Bonenfant et al., 2009; Toïgo et al., 2006). Although
662 593 there is no official estimate of the population density at Gouaro-Déva, the recovery of
663 594 vegetation in the area and an improved body shape condition of the deer in recent years testify
664 595 to the sharp decline in the density of this "natural disaster" since the introduction of the jawbone
665 596 reward in 2008, designed to protect endemic New-Caledonian flora and fauna from the
666 597 destruction caused by this invasive deer. An increasing number of studies are examining the
667 598 impact of human-related disturbances on animal behaviour (Frid and Dill, 2002). Greater animal
668 599 mobility in response to human disturbance could limit access to resources (Frid and Dill, 2002;
669 600 Jayakody et al., 2011), thereby impacting animal growth and adult size. At Gouaro-Déva, human
670 601 recreational activities occur on a daily basis throughout the year (hiking, horse riding, 4x4
671 602 excursions, hunting, golf, etc.) and deer mobility is much more important than in other habitats
672 603 (Berlioz, *Pers. Obs.*). Therefore, we propose that the small size of the rusa deer at Gouaro Déva
673 604 is the result of higher levels of stress for these animals. Despite the availability of resources, the
674 605 animals spend more time in constant displacements, and less time foraging. This negative effect
675 606 of stress has previously been demonstrated in a population of mouflon in Southern Spain (Azorit
676 607 et al., 2020), where it resulted in poor ontogenic development associated with delayed tooth
677 608 eruption and a smaller, more gracile adult mandible. As a result, these animals were less able to
678 609 process hard food. This hypothesis could be tested by conducting an ontogenic study on rusa
679 610 deer mandibles from the biological collections of the University of Poitiers.

680 611 The morphologies of the mandibular bones of rusa deer from the Gouaro-Déva and Grandes
681 612 Fougères provincial parks clearly differ, partly attributable to the very contrasting vegetation
682 613 between these two habitats. The Grandes Fougères Provincial Park is indeed 90% dense tropical

684 614 rainforest. A high density of deer exploits a few meadows and grassy areas along the tracks and
685 615 parkings, but the deer also browse intensively on the woody vegetation of the park, causing
686 616 major damage to ligneous plants (Berlioz, *pers. obs.*). On the other side, while the Gouaro Déva
687 617 domain includes an important relic of the New Caledonian dry forest, its primary vegetation is
688 618 large areas of niaouli savannah, characterised by an abundant herbaceous layer rich in
689 619 monocotyledons.

690 620 The angular process of the mandible of the deer from the Grandes Fougères Provincial Park is
691 621 prominent. This area corresponds to the insertion zone of the masseter muscle on the labial side
692 622 and the pterygoid muscle on the buccal side (Pérez-Barbería and Gordon, 1999). The coronoid
693 623 process, where the temporalis muscle is inserted, is longer and wider. The robustness of the
694 624 mandibles of these deer meets high biomechanical requirements. Indeed, these animals feed
695 625 on tough vegetal resources like tree fern fronds (Berlioz, *pers. obs.*), requiring substantial biting
696 626 force to be comminuted. Le Cap and Misère are characterised by more abundant herbaceous
697 627 layers and more open landscapes compared to the Grandes Fougères Provincial Park, and the
698 628 morphology of their mandibles shows intermediate values, with slightly greater similarities to
699 629 the Gouaro Déva deer.

700 630 Our results offer a clearer understanding of the relationships between mandible size, variations
701 631 in mandibular bone morphology, the impact of environmental and genetic factors. By exploring
702 632 the mandibular morphology of these two present-day cervids living under well-known
703 633 environmental conditions, this study will provide a benchmark for studying fossil specimens for
704 634 which environmental and genetic data are generally scarce or unavailable. This study
705 635 demonstrates the advantages of studying mandibular morphology for palaeoecological and
706 636 palaeoenvironmental reconstructions.

708 637 **Conclusion**

709 638 We have provided evidence supporting the idea that although taxonomy significantly influences
710 639 variations in mandibular bone morphology between species, this morphology is likely to provide
711 640 valuable insights into the ecology and environment of species at a finer scale, both within and
712 641 among populations. We have shown a linear relationship between the robustness of the
713 642 mandibles of European red deer and the latitude along a North-South aridification gradient.
714 643 While such a relationship had already been shown for moose (Kangas et al., 2017), it had never
715 644 been demonstrated for red deer populations on such a large geographical scale. These
716 645 differences in shape can be linked to the biomechanical forces required to process food, the
717 646 physical properties of which vary between climatic regions. These interesting results
718 647 demonstrate the potential of mandibular bone morphology as an eco-indicator to track the
719 648 responses of ungulates to the current trend of aridification and even desertification in Europe,
720 649 particularly concerning for the Iberian, Italian and Balkan peninsulas, as well as Eastern Europe,
721 650 in the context of global climate change (Gao and Giorgi, 2008; Polade et al., 2014).

722 651 Since there is only one genetically homogeneous population of rusa deer in New Caledonia
723 652 (Frantz et al., 2024), this constitutes a unique model for studying the relationship between
724 653 morphology and environmental factors. This particularity has enabled us to delve deeper into
725 654 this question and to suggest the impact of other factors on this mandibular shape variation, such
726 655 as stress induced by human activities. This work also makes a valuable contribution to our
727 656 knowledge of the New Caledonian rusa deer, an invasive species whose management is essential
728 657 to protecting this biodiversity hotspot but whose ecology and plasticity are paradoxically still
729 658 insufficiently documented. It has also enabled us to identify interesting new research
730 659 perspectives.

731 660 Finally, our findings also emphasize the potential of studying well-preserved fossil deer
732 661 mandibles to contribute to our understanding of palaeoenvironments, their evolution over time,

734 662 and the ecological responses of fossil species to environmental changes induced by past climatic
735 663 oscillations.

736 664 **Acknowledgements:**

737 665 This work is dedicated to the memory of Professor Concepción Azorit, a brilliant scientist and
738 666 cherished colleague whose enthusiasm and commitment greatly contributed to this study. Her
739 667 passion for science will continue to inspire us.

740 668 For the New Caledonian material, we are grateful to the numerous persons who provided their
741 669 valuable assistance during fieldwork. We would like to thank the southern New Caledonian
742 670 province, the Institut Agronomic Néo-Calédonien, the Agence Rurale, the DR8 of the Center
743 671 national de la recherche scientifique (CNRS), Mr Philippe Severian, Director of the Direction du
744 672 Développement Rural-Province Sud, and Mr Lionnel Brinon, Director of the Agence pour
745 673 prevention and compensation for agricultural or natural disasters (Apican) and President of the
746 674 Agence Rurale, who all supported the "DMTA Rusa" project. We also thank Palévoprim Lab,
747 675 Gildas Merceron and Marc Colyn for their contribution to this project. Some of the samples were
748 676 provided by the GEE of the "Conservatoire des Espaces Naturels". Concerning the *Cervus elaphus*
749 677 jaws from the El Durazno hunting reserve in Argentina, we would like to thank Diego Torres for
750 678 his help in collecting them. We thank the Palévoprim laboratory for access to material from the
751 679 Hemne, Broceliande and New Caledonian populations. For the Pyrenean samples, we are
752 680 grateful to the staff from both the National Hunting Reserves and the Generalitat de Catalunya.
753 681 Finally, the authors thank the 'Organismo Autónomo de Parques Nacionales, Ministerio de
754 682 Medio Ambiente, Medio Rural y Marino', and the University of Jaén, Spain, for their support in
755 683 providing the necessary material and access to grounds for this study, to the project PID2022-
756 684 1426610B-I00, granted by the Ministerio de Ciencia e Innovación, Spain, as well as the
757 685 INVESTIGO Program the SEPE, Ministerio de Trabajo y Economía Social, Spain (Resolution, Order
758 686 TES/1267/2021).

759 687

References

- 761 688 **References**
- 762 689 Adams, S.D., Collyer, M., Kaliontzopoulou, A., Baken, E.K., 2024. Geomorph: Software for
763 690 geometric morphometric analyses. R package version 4.0.7.
- 764 691 Albon, S.D., Langvatn, R., 1992. Plant phenology and the benefits of migration in a temperate
765 692 ungulate. *Oikos* 65, 502–513.
- 766 693 Anderson, D.L., 1979. La distribución de *Sorghastrum pellitum* (Poaceae) en la provincia de San
767 694 Luis y su significado ecológico. *Kurtziana* 12e13, 37e45.
- 768 695 Anderson, D.L., del Aguila, J.A., Bernardon, A.E., 1970. Las formaciones vegetales en la
769 696 provincia de San Luis. INTA.
- 770 697 Arenzana, O., Rodríguez, F.G., Sanchez, J.L.F., 1965. Repoblaciones de caza mayor. Ministerio
771 698 de Agricultura. Dirección General de Monte, Caza y Pesca Fluvial ...
- 772 699 Aune, E.I., 1973. Forest vegetation in Hemne, Sør-Trøndelag, Western Central Norway, K.
773 700 norske Vidensk. Selsk. Mus. Miscellanea. NTNU Vitenskapsmuseet.
- 774 701 Azorit, C., Analla, M., Muñoz-Cobo, J., 2003. Variation of mandible size in red deer *Cervus*
775 702 *elaphus hispanicus* from southern Spain. *Acta Theriol* 48, 221–228.
776 703 <https://doi.org/10.1007/BF03194161>
- 777 704 Azorit, C., Jimenez Tenorio, M., Casinos, A., Lopez Montoya, A.J., Lopez-Fuster, M.J., Rocha
778 705 Barbosa, O., 2020. Searching for indicators of age, sex and population in European
779 706 mouflon mandibles.
- 780 707 Azorit, C., Tellado Ruiz, M.S., Oya, A., Moro, J., 2012. Seasonal and specific diet variations in
781 708 sympatric red and fallow deer of southern Spain: a preliminary approach to feeding
782 709 behaviour. *Animal Production Science* 52, 720–727.
- 783 710 Baken, E.K., Collyer, M.L., Kaliontzopoulou, A., Adams, D.C., 2021. geomorph v4.0 and
784 711 gmShiny: Enhanced analytics and a new graphical interface for a comprehensive
785 712 morphometric experience. *Methods Ecol Evol* 12, 2355–2363.
786 713 <https://doi.org/10.1111/2041-210X.13723>
- 787 714 Barrau, J., Devambe, L., 1957. Quelques résultats inattendus de l'acclimatation en Nouvelle-
788 715 Calédonie. *La Terre et la vie*.
- 789 716 Berlioz, E., 2017. Écologie alimentaire et paléoenvironnements des cervidés européens du
790 717 Pléistocène inférieur : le message des textures de micro-usure dentaire (PhD Thesis).
791 718 Université de Poitiers, France.
- 792 719 Berlioz, E., Azorit, C., Blondel, C., Tellado Ruiz, M.S., Merceron, G., 2017. Deer in an arid
793 720 habitat: dental microwear textures track feeding adaptability. *Hystrix, the Italian*
794 721 *Journal of Mammalogy* 28, 222–230.
- 795 722 Berlioz, E., Merceron, G., Colyn, M., 2020. Le cerf rusa, espèce invasive: Micro-usure dentaire,
796 723 écologies inter et intra-populationnelles, régime alimentaire, génétique des paysages.
797 724 Laboratoire PALEVOPRIM.
- 798 725 Berton, J.A., Echeverría, J.C., 1999. Cambio climático global en San Luis: Régimen
799 726 pluviométrico. VII Jornadas Cuidemos Nuestro Mundo. Universidad Nacional de San
800 727 Luis, San Luis 48–50.
- 801 728 Bonenfant, C., Gaillard, J.-M., Coulson, T., Festa-Bianchet, M., Loison, A., Garel, M., Loe, L.E.,
802 729 Blanchard, P., Pettorelli, N., Owen-Smith, N., 2009. Empirical evidence of density-
803 730 dependence in populations of large herbivores. *Advances in ecological research* 41,
804 731 313–357.
- 805 732 Bugalho, M.N., Milne, J.A., 2003. The composition of the diet of red deer (*Cervus elaphus*) in a
806 733 Mediterranean environment: a case of summer nutritional constraint? *Forest Ecology*
807 734 *and Management* 181, 23–29.
- 808 735 Carranza, J., Salinas, M., De Andrés, D., Pérez-González, J., 2016. Iberian red deer: paraphyletic
809 736 nature at mt DNA but nuclear markers support its genetic identity. *Ecology and*
810 737 *Evolution* 6, 905–922. <https://doi.org/10.1002/ece3.1836>

- 812 738 Clauss, M., Hofmann, R.R., Streich, W.J., Fickel, J., Hummel, J., 2008. Higher masseter muscle
813 739 mass in grazing than in browsing ruminants. *Oecologia* 157, 377–385.
814 740 <https://doi.org/10.1007/s00442-008-1093-z>
- 815 741 Croitor, R., 2018. Plio-Pleistocene deer of western Palearctic: taxonomy, systematics,
816 742 phylogeny. Institute of Zoology of the Academy of Sciences of Moldova.
- 817 743 Currey, J.D., 2003. The many adaptations of bone. *Journal of Biomechanics* 36, 1487–1495.
- 818 744 De Felice, E., Pacioni, C., Tardella, F.M., Dall'Aglio, C., Palladino, A., Scocco, P., 2020. A Novel
819 745 Method for Increasing the Numerousness of Biometrical Parameters Useful for Wildlife
820 746 Management: Roe Deer Mandible as Bone Model. *Animals* 10, 465.
- 821 747 Deinum, B., 1981. The influence of physical factors on the nutrient content of forages.
822 748 Veenman.
- 823 749 Dellicour, S., Frantz, A.C., Colyn, M., Bertouille, S., Chaumont, F., Flamand, M.-C., 2011.
824 750 Population structure and genetic diversity of red deer (*Cervus elaphus*) in forest
825 751 fragments in north-western France. *Conservation Genetics* 12, 1287–1297.
- 826 752 Dinerstein, E., Olson, D., Joshi, A., Vynne, C., Burgess, N.D., Wikramanayake, E., Hahn, N.,
827 753 Palminteri, S., Hedao, P., Noss, R., 2017. An ecoregion-based approach to protecting
828 754 half the terrestrial realm. *BioScience* 67, 534–545.
- 829 755 Fletcher, T.M., Janis, C.M., Rayfield, E.J., 2010. Finite element analysis of ungulate jaws: can
830 756 mode of digestive physiology be determined. *Palaeontologia Electronica* 13, 1–15.
- 831 757 Frantz, A.C., Luttringer, A., Colyn, M., Kazila, C., Berlioz, E., 2024. Landscape structure does not
832 758 hinder the expansion of an invasive herbivorous mammal in the New Caledonian
833 759 Biodiversity hotspot. *European journal of wildlife research management of alien*
834 760 *species*.
- 835 761 Frid, A., Dill, L., 2002. Human-caused disturbance stimuli as a form of predation risk.
836 762 *Conservation Ecology* 6, 1–16.
- 837 763 Gao, X., Giorgi, F., 2008. Increased aridity in the Mediterranean region under greenhouse gas
838 764 forcing estimated from high resolution simulations with a regional climate model.
839 765 *Global and Planetary Change* 62, 195–209.
- 840 766 Gargominy, O., Bouchet, P., Pascal, M., Jaffré, T., Tourneur, J.-C., 1996. Conséquences des
841 767 introductions d'espèces animales et végétales sur la biodiversité en Nouvelle-
842 768 Calédonie. *Revue d'Ecologie, Terre et Vie* 51, 375–402.
- 843 769 Gębczyńska, Z., 1980. Food of the roe deer and red deer in the Białowieża Primeval Forest.
844 770 *Acta Theriologica* 25, 487–500.
- 845 771 Gebert, C., Verheyden-Tixier, H., 2001. Variations of diet composition of red deer (*Cervus*
846 772 *elaphus* L.) in Europe. *Mammal Review* 31, 189–201.
- 847 773 Geist, V., 1998. *Deer of the world: their evolution, behaviour, and ecology*. Stackpole books.
- 848 774 Gort-Esteve, A., Riera, J.L., Ruiz-Olmo, J., Pérez-Haase, A., Filella, J.B., 2023. Diet Composition
849 775 and Habitat Use by Red Deer in Two Rewilded Mountain Areas. *International Journal of*
850 776 *Zoology and Animal Biology* 6, Volume-6.
- 851 777 Greaves, W.S., 1991. The orientation of the force of the jaw muscles and the length of the
852 778 mandible in mammals. *Zoological Journal of the Linnean Society* 102, 367–374.
- 853 779 Hammer, Ø., Harper, D.A.T., 2008. *Paleontological data analysis*. John Wiley & Sons.
- 854 780 Hebblewhite, M., Merrill, E., McDermid, G., 2008. A multi-scale test of the forage maturation
855 781 hypothesis in a partially migratory ungulate population. *Ecological Monographs* 78,
856 782 141–166. <https://doi.org/10.1890/06-1708.1>
- 857 783 Hedges, S.B., Duckworth, J.W., Timmins, R.S., Semiadi, G., Priyono, A., 2008. *Rusa timorensis*.
- 858 784 Hewitt, G.M., 1999. Post-glacial re-colonization of European biota. *Biological journal of the*
859 785 *Linnean Society* 68, 87–112.
- 860 786 Jaksic, F.M., Iriarte, J.A., Jiménez, J.E., Martínez, D.R., 2002. Invaders without frontiers: cross-
861 787 border invasions of exotic mammals. *Biological Invasions* 4, 157–173.
862 788 <https://doi.org/10.1023/A:1020576709964>

- 864 789 Janis, C.M., 1995. Correlations between craniodental morphology and feeding behavior in
865 790 ungulates: reciprocal illumination between living and fossil taxa. *Functional*
866 791 *morphology in vertebrate paleontology* 76–98.
- 867 792 Jayakody, S., Sibbald, A.M., Mayes, R.W., Hooper, R.J., Gordon, I.J., Lambin, X., 2011. Effects of
868 793 human disturbance on the diet composition of wild red deer (*Cervus elaphus*). *Eur J*
869 794 *Wildl Res* 57, 939–948. <https://doi.org/10.1007/s10344-011-0508-z>
- 870 795 Jones, J.R., Marín-Arroyo, A.B., Straus, L.G., Richards, M.P., 2020. Adaptability, resilience and
871 796 environmental buffering in European Refugia during the Late Pleistocene: Insights
872 797 from La Riera cave (Asturias, cantabria, Spain). *Scientific Reports* 10, 1–17.
- 873 798 Kangas, V.-M., Rytönen, S., Kvist, L., Käpylä, T., Nygrén, T., Aspi, J., 2017. Geographic cline in
874 799 the shape of the moose mandible: indications of an adaptive trend. *Journal of*
875 800 *Mammalian Evolution* 24, 233–241.
- 876 801 Kelly, C.L., Gordon, I.J., Schwarzkopf, L., Pintor, A., Pople, A., Hirsch, B.T., 2023. Invasive wild
877 802 deer exhibit environmental niche shifts in Australia: Where to from here? *Ecology and*
878 803 *Evolution* 13, e10251. <https://doi.org/10.1002/ece3.10251>
- 879 804 Klein, F., 1990. La réintroduction du cerf *Cervus elaphus*. *Revue d'Écologie* 131–134.
- 880 805 Langvatn, R., Albon, S.D., 1986. Geographic clines in body weight of Norwegian red deer: a
881 806 novel explanation of Bergmann's rule? *Ecography* 9, 285–293.
882 807 <https://doi.org/10.1111/j.1600-0587.1986.tb01221.x>
- 883 808 Langvatn, R., Hanley, T.A., 1993. Feeding-patch choice by red deer in relation to foraging
884 809 efficiency: An experiment. *Oecologia* 95, 164–170.
885 810 <https://doi.org/10.1007/BF00323486>
- 886 811 Latham, A.D.M., Nugent, G., 2017. Introduction, impacts, and management of non-native deer
887 812 and other hunted ungulates in New Zealand. *Journal of Japan Deer Studies* 2017, 41–
888 813 57.
- 889 814 Lawing, A.M., Polly, P.D., 2010. Geometric morphometrics: recent applications to the study of
890 815 evolution and development. *Journal of Zoology* 280, 1–7.
- 891 816 Lister, A.M., 1996. The morphological distinction between bones and teeth of fallow deer
892 817 (*Dama dama*) and red deer (*Cervus elaphus*). *International Journal of*
893 818 *Osteoarchaeology* 6, 119–143.
- 894 819 Lovari, S., Lorenzini, R., Masseti, M., Pereladova, O., Carden, R.F., Brook, S.M., Mattioli, S.,
895 820 2018. *Cervus elaphus* [WWW Document]. The IUCN Red List of Threatened Species.
- 896 821 Mackiewicz, P., Matosiuk, M., Świsłocka, M., Zachos, F.E., Hajji, G.M., Saveljev, A.P., Seryodkin,
897 822 I.V., Farahvash, T., Rezaei, H.R., Torshizi, R.V., 2022. Phylogeny and evolution of the
898 823 genus *Cervus* (Cervidae, Mammalia) as revealed by complete mitochondrial genomes.
899 824 *Scientific Reports* 12, 16381.
- 900 825 Marañón, T., 1991. Diversidad en comunidades de pasto mediterráneo: modelos y
901 826 mecanismos de coexistencia. *Ecología* 5, 149–157.
- 902 827 McNab, B.K., 2010. Geographic and temporal correlations of mammalian size reconsidered: a
903 828 resource rule. *Oecologia* 164, 13–23. <https://doi.org/10.1007/s00442-010-1621-5>
- 904 829 Meiri, M., Lister, A.M., Higham, T.F., Stewart, J.R., Straus, L.G., Obermaier, H., Gonzalez
905 830 Morales, M.R., Marín-Arroyo, A.B., Barnes, I., 2013. Late-glacial recolonization and
906 831 phylogeography of European red deer (*Cervus elaphus* L.). *Molecular Ecology* 22,
907 832 4711–4722.
- 908 833 Merceron, G., Escarguel, G., Angibault, J.-M., Verheyden-Tixier, H., 2010. Can dental microwear
909 834 textures record inter-individual dietary variations? *PLoS ONE* 5, 1–9.
- 910 835 Merino, M.L., Carpinetti, B.N., Abba, A.M., 2009. Invasive mammals in the national parks
911 836 system of Argentina. *Natural Areas Journal* 29, 42–49.
- 912 837 Mittermeier, R.A., Turner, W.R., Larsen, F.W., Brooks, T.M., Gascon, C., 2011. Global
913 838 biodiversity conservation: the critical role of hotspots, in: *Biodiversity Hotspots*.
914 839 Springer, pp. 3–22.

- 916 840 MNHN Natura 2000, 2017. INPN - FSD Natura 2000 - FR5300005 - Forêt de Paimpont -
917 841 Description [WWW Document]. URL <https://inpn.mnhn.fr/site/natura2000/FR5300005>
918 842 (accessed 5.10.24).
- 919 843 Myers, N., Mittermeier, R.A., Mittermeier, C.G., Da Fonseca, G.A., Kent, J., 2000. Biodiversity
920 844 hotspots for conservation priorities. *Nature* 403, 853–858.
- 921 845 Mysterud, A., 2000. Diet overlap among ruminants in Fennoscandia. *Oecologia* 124, 130–137.
922 846 <https://doi.org/10.1007/s004420050032>
- 923 847 Neaux, D., Blanc, B., Ortiz, K., Locatelli, Y., Laurens, F., Baly, I., Callou, C., Lecompte, F.,
924 848 Cornette, R., Sansalone, G., 2021. How changes in functional demands associated with
925 849 captivity affect the skull shape of a wild boar (*Sus scrofa*). *Evolutionary Biology* 48, 27–
926 850 40.
- 927 851 Neaux, D., Louail, M., Ferchaud, S., Surault, J., Merceron, G., 2022. Experimental assessment of
928 852 the relationship between diet and mandibular morphology using a pig model: New
929 853 insights for paleodietary reconstructions. *The Anatomical Record* ar.24895.
930 854 <https://doi.org/10.1002/ar.24895>
- 931 855 Niedziałkowska, M., Jędrzejewska, B., Honnen, A.-C., Otto, T., Sidorovich, V.E., Perzanowski, K.,
932 856 Skog, A., Hartl, G.B., Borowik, T., Bunevich, A.N., Lang, J., Zachos, F.E., 2011. Molecular
933 857 biogeography of red deer *Cervus elaphus* from eastern Europe: insights from
934 858 mitochondrial DNA sequences. *Acta Theriol* 56, 1–12. [https://doi.org/10.1007/s13364-](https://doi.org/10.1007/s13364-010-0002-0)
935 859 010-0002-0
- 936 860 Novillo, A., Ojeda, R.A., 2008. The exotic mammals of Argentina. *Biol Invasions* 10, 1333–1344.
937 861 <https://doi.org/10.1007/s10530-007-9208-8>
- 938 862 Ozaki, M., Suwa, G., Kaji, K., Ohba, T., Hosoi, E., Koizumi, T., Takatsuki, S., 2007. Correlations
939 863 between feeding type and mandibular morphology in the sika deer. *Journal of Zoology*
940 864 272, 244–257. <https://doi.org/10.1111/j.1469-7998.2006.00264.x>
- 941 865 Ozenda, P., Borel, J.-L., 2000. An ecological map of Europe: why and how? *Comptes Rendus de*
942 866 *l'Académie des Sciences-Series III-Sciences de la Vie* 323, 983–994.
- 943 867 Paschetta, C., de Azevedo, S., Castillo, L., Martínez-Abadías, N., Hernández, M., Lieberman,
944 868 D.E., González-José, R., 2010. The influence of masticatory loading on craniofacial
945 869 morphology: A test case across technological transitions in the Ohio valley. *American*
946 870 *Journal of Physical Anthropology: The Official Publication of the American Association*
947 871 *of Physical Anthropologists* 141, 297–314.
- 948 872 Peel, M.C., Finlayson, B.L., McMahon, T.A., 2007. Updated world map of the Köppen-Geiger
949 873 climate classification. *Hydrology and earth system sciences discussions* 4, 439–473.
- 950 874 Pérez-Barbería, F.J., Gordon, I.J., 1999. The functional relationship between feeding type and
951 875 jaw and cranial morphology in ungulates. *Oecologia* 118, 157–165.
- 952 876 Pérez-González, J., Gort-Esteve, A., Ruiz-Olmo, J., Anaya, G., Broggin, C., Millán, M.F., Vedel,
953 877 G., De La Peña, E., Membrillo, A., Seoane, J.M., Azorit, C., Carranza, J., 2023. Red deer
954 878 in the Pyrenees: a risky secondary contact zone for conservation genetics. *J Wildl*
955 879 *Manag* 87, e22454. <https://doi.org/10.1002/jwmg.22454>
- 956 880 Polade, S.D., Pierce, D.W., Cayan, D.R., Gershunov, A., Dettinger, M.D., 2014. The key role of
957 881 dry days in changing regional climate and precipitation regimes. *Scientific reports* 4, 1–
958 882 8.
- 959 883 Pordomingo, A.J., Rucci, T., 2000. Red deer and cattle diet composition in La Pampa, Argentina.
960 884 *Rangeland Ecology & Management/Journal of Range Management Archives* 53, 649–
961 885 654.
- 962 886 Raia, P., Carotenuto, F., Meloro, C., Piras, P., Pushkina, D., 2010. The shape of contention:
963 887 adaptation, history, and contingency in ungulate mandibles. *Evolution* 64, 1489–1503.
- 964 888 Rohlf, F.J., 2021. TpsDig2, <https://www.sbmorphometrics.org/index.html>.
- 965 889 Savouré-Soubelet, A., Arthur, C.-P., Aulagnier, S., Body, G., Callou, C., Haffner, P.,
966 890 Marchandeu, S., Moutou, F., Saint-Andrieux, C., 2021. Atlas des mammifères

- 968 891 sauvages de France. Volume 2: Ongulés et Lagomorphes. Muséum national d'Histoire
969 892 naturelle.
- 970 893 Seilacher, A., 1970. Arbeitskonzept zur konstruktions-morphologie. LET 3, 393–396.
971 894 <https://doi.org/10.1111/j.1502-3931.1970.tb00830.x>
- 972 895 Sheets, H.D., 2014. Integrated morphometrics package (IMP) 8. <http://www2.canisius.edu/~>
973 896 sheets.
- 974 897 Skog, A., Zachos, F.E., Rueness, E.K., Feulner, P.G.D., Mysterud, A., Langvatn, R., Lorenzini, R.,
975 898 Hmwe, S.S., Lehoczy, I., Hartl, G.B., Stenseth, N.C., Jakobsen, K.S., 2009.
976 899 Phylogeography of red deer (*Cervus elaphus*) in Europe. Journal of Biogeography 36,
977 900 66–77. <https://doi.org/10.1111/j.1365-2699.2008.01986.x>
- 978 901 Spencer, L.M., 1995. Morphological correlates of dietary resource partitioning in the African
979 902 Bovidae. Journal of Mammalogy 76, 448–471.
- 980 903 Taberlet, P., Fumagalli, L., WUST-SAUCY, A.-G., COSSON, J.-F., 1998. Comparative
981 904 phylogeography and postglacial colonization routes in Europe. Molecular ecology 7,
982 905 453–464.
- 983 906 Terada, C., Tatsuzawa, S., Saitoh, T., 2012. Ecological correlates and determinants in the
984 907 geographical variation of deer morphology. Oecologia 169, 981–994.
985 908 <https://doi.org/10.1007/s00442-012-2270-7>
- 986 909 Toïgo, C., Gaillard, J.-M., Van Laere, G., Hewison, M., Morellet, N., 2006. How does
987 910 environmental variation influence body mass, body size, and body condition? Roe deer
988 911 as a case study. Ecography 29, 301–308.
- 989 912 Varela, L., Fariña, R.A., 2015. Masseter moment arm as a dietary proxy in herbivorous
990 913 ungulates. Journal of Zoology 296, 295–304. <https://doi.org/10.1111/jzo.12246>
- 991 914 Verheyden-Tixier, H., Renaud, P.-C., Morellet, N., Jamot, J., Besle, J.-M., Dumont, B., 2008.
992 915 Selection for nutrients by red deer hinds feeding on a mixed forest edge. Oecologia
993 916 156, 715–726.
- 994 917 Wang, B., Zelditch, M., Badgley, C., 2022. Geometric morphometrics of mandibles for dietary
995 918 differentiation of Bovidae (Mammalia: Artiodactyla). Current Zoology 68, 237–249.
- 996 919 Wolff, J., 1892. Das Gesetz der Transformation der Knochen, Berlin, A. Hirschwald. The Law of
997 920 Bone Remodeling, Hirschwald XII, 152 p.
- 998 921 Zachos, F.E., Frantz, A.C., Kuehn, R., Bertouille, S., Colyn, M., Niedziałkowska, M., Pérez-
999 922 González, J., Skog, A., Sprēm, N., Flamand, M.-C., 2016. Genetic structure and effective
1000 923 population sizes in European red deer (*Cervus elaphus*) at a continental scale: insights
1001 924 from microsatellite DNA. Journal of Heredity 107, 318–326.
- 1002 925 Zelditch, M.L., Swiderski, D.L., Sheets, H.D., 2012. Geometric morphometrics for biologists: a
1003 926 primer. Academic Press.
- 1004 927 Zhou, Z., Winkler, D.E., Fortuny, J., Kaiser, T.M., Marcé-Nogué, J., 2019. Why ruminating
1005 928 ungulates chew sloppily: biomechanics discern a phylogenetic pattern. PLoS One 14,
1006 929 e0214510.
- 1007 930

| | | |
|------|-----|--|
| 1009 | 931 | Tables, Figures, Supplementary data: |
| 1010 | 932 | Tables and SI Tables |
| 1011 | 933 | Table1: Information on the habitats of cervid populations. Information on biomes is taken |
| 1012 | 934 | from https://ecoregions.appspot.com/ . Description of the local vegetation for the populations |
| 1013 | 935 | living in geographical Europe is taken from Ozenda & Borel, 2000. For El Durazno and the Neo- |
| 1014 | 936 | Caledonian localities, the description is based on field observations. |
| 1015 | 937 | Table 2: Description of landmarks and semilandmarks used for capturing the mandibular shape |
| 1016 | 938 | <i>for the geometric morphometric analysis.</i> |
| 1017 | 939 | Table S1: results of ANOVA analyses (p-values) |
| 1018 | 940 | Table S2: results of Duncan post-hoc tests |
| 1019 | 941 | Table S3: results of procrust regressions evaluating how mandible shape vary as a function of |
| 1020 | 942 | size and species (for Cervini), population (for <i>C. elaphus</i>) and habitat (for <i>R. timorensis</i>). |
| 1021 | 943 | Table S4: results of procrust regressions (p-values and R ²) for each axis of PCA carrying |
| 1022 | 944 | significant interpopulation and inter-habitat differences. |
| 1023 | 945 | Table S5: results of Partial Least Squares |
| 1024 | 946 | |
| 1025 | 947 | Figures |
| 1026 | 948 | Figure 1: Location of the eight Cervini populations included in the study. <i>Cervus elaphus</i> : El |
| 1027 | 949 | Durazno, Hemne, Broceliande, Alt Pallars, Boumort, Selladores, Valquemado. <i>Rusa timorensis</i> : |
| 1028 | 950 | New Caledonia (Gouaro Déva, Le Cap, Misère, Parc des Grandes Fougères (PGF)). |
| 1029 | 951 | Figure 2: Landmarks (blue) and semi-landmarks (black) used to capture the mandibular bone |
| 1030 | 952 | morphology through a 2D geometric morphometric analysis on the buccal side of the left |
| 1031 | 953 | hemimandible. A: mandible of a red deer specimen from the Selladores-Contadero population. |
| 1032 | 954 | B: Consensus shape for <i>Cervus elaphus</i> . The anatomical structures and regions corresponding to |
| 1033 | 955 | numbers 1-40 are described in Table 2. |
| 1034 | 956 | Figure 3: Biplot representing the two first principal components of the PCA exploring |
| 1035 | 957 | interspecific mandibular shape variations between <i>Cervus elaphus</i> and <i>Rusa timorensis</i> . Shape |
| 1036 | 958 | deformations are shown along PC1 and 2 for each species (<i>C. elaphus</i> : coral; <i>R. timorensis</i> : navy |
| 1037 | 959 | blue). The consensus shape for all Cervini is shown in grey to aid interpretation. |
| 1038 | 960 | Figure 4: A: Biplot representing the two first principal components of the PCA (63.3% of the |
| 1039 | 961 | variance) exploring <i>Cervus elaphus</i> interpopulation mandibular shape variations. Shape |
| 1040 | 962 | deformations are shown along PC1 and 2 for each population (Alt Pallars: pink; Boumort: red; |
| 1041 | 963 | Broceliande: mauve; El Durazno: green; Hemne: purple; Selladores: dark yellow; Valquemado: |
| 1042 | 964 | orange). The consensus shape for all <i>C. elaphus</i> is in grey to aid interpretation. B: Focus on the |
| 1043 | 965 | variation on PC1. Letters (a-e) represent interpopulation differences based on Duncan post hoc |
| 1044 | 966 | test. C: Biplot representing the two first canonical variates of the CVA. |

1046 967 **Figure 5:** A: Biplot representing the two first principal components of the PCA (47.76% of the
1047 968 variance) exploring *Rusa timorensis* intrapopulation mandibular shape variations between
1048 969 contrasting habitats. Shape deformations are shown along PC1 and 2 for each population
1049 970 (Gouaro Déva: Turquoise, Le Cap: royal blue, Misère: plum, Parc des Grandes Fougères (PGF):
1050 971 navy blue). The consensus shape for all *R. timorensis* is in grey to aid interpretation. B: Focus on
1051 972 the variation on PC2. Letters a and b represent interpopulation differences based on Duncan's
1052 973 post hoc test. C: Biplot representing the two first canonical variates of the CVA.

1053 974 **Figure 6:** Allometric relationships and morphological variation in *Cervus elaphus* from different
1054 975 populations (A) and *Rusa timorensis* from contrasted local habitats (B). Plots illustrate body size
1055 976 and shape variations, both within and among Cervini populations, highlighting population-
1056 977 specific morphological trends. Log(Size): log-transformed body size; CAC and RSC1 are
1057 978 morphological metrics. CAC: Common Allometric Component; RSC1: Residual Shape Component
1058 979 1; PC1: Principal Component 1. The rightmost plots provide information regarding allometry or
1059 980 isometry.

1060 981

1061 982 **Supplementary data**

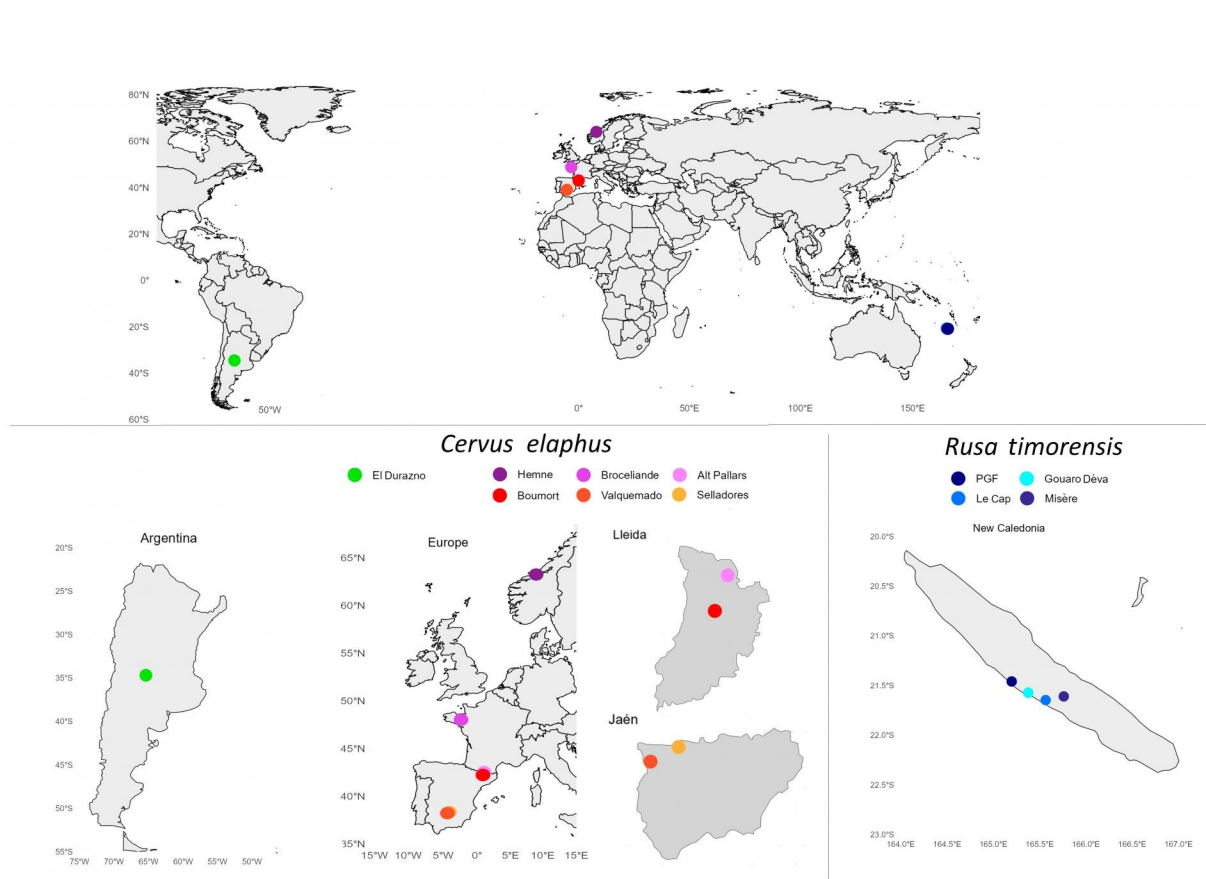
1062 983 **Annex 1:** R script (R Markdown)

Table 1: Information on the habitats of cervid populations. Information on biomes is taken from <https://ecoregions.appspot.com/>. Description of the local vegetation for the populations living in geographical Europe is taken from Ozenda and Borel, 2000. For El Durazno and the Neo-Caledonian localities, the description is based on field observations.

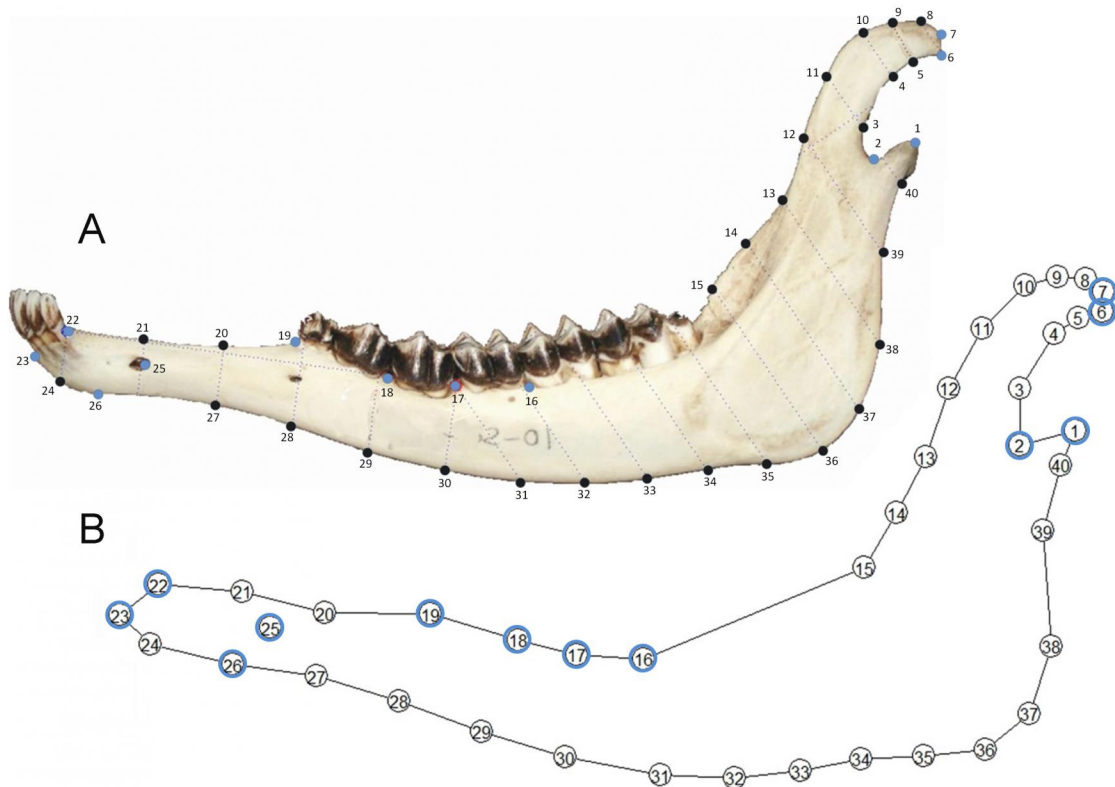
| | Group | Biome | Local vegetation description |
|------------------------|---------------------------|--|--|
| <i>Cervus elaphus</i> | Alt Pallars | Temperate Broadleaf & Mixed Forests | High mountain: subalpine, alpine and nival vegetation belts |
| | Boumort | Temperate Broadleaf & Mixed Forests | Lower and mid-mountain: collinean and montane vegetation belts |
| | Broceliande (Paimpont) | Temperate Broadleaf & Mixed Forests | Hyperhygrophilous Armorican sector |
| | El Durazno | Temperate Grasslands, Savannas & Shrublands | Semiarid Pampas |
| | Hemne | Boreal Forests/Taiga | Orocaledonian vegetation unit (mountain tundra) |
| | Selladores | Mediterranean Forests, Woodlands & Scrub | Siliceous, with round-leaved oak |
| | Valquemado | Mediterranean Forests, Woodlands & Scrub | Calicolous, with round-leaved oak |
| <i>Rusa timorensis</i> | Gouaro Déva | Tropical & Subtropical Dry Broadleaf Forests | Sclerophyllous & meso-sclerophyll forests, extensive grasslands, Niaoulis savannah |
| | Le Cap | Tropical & Subtropical Dry Broadleaf Forests | Niaoulis savannah & agricultural grasslands |
| | Misère | Tropical & Subtropical Dry Broadleaf Forests | Mesophyll forest |
| | Parc des Grandes Fougères | Tropical & Subtropical Moist Broadleaf Forests | Dense tropical rainforest |

Table 2. Labial view of a left deer mandible and description of landmarks and semilandmarks used for capturing the mandibular shape for the geometric morphometric analyses.

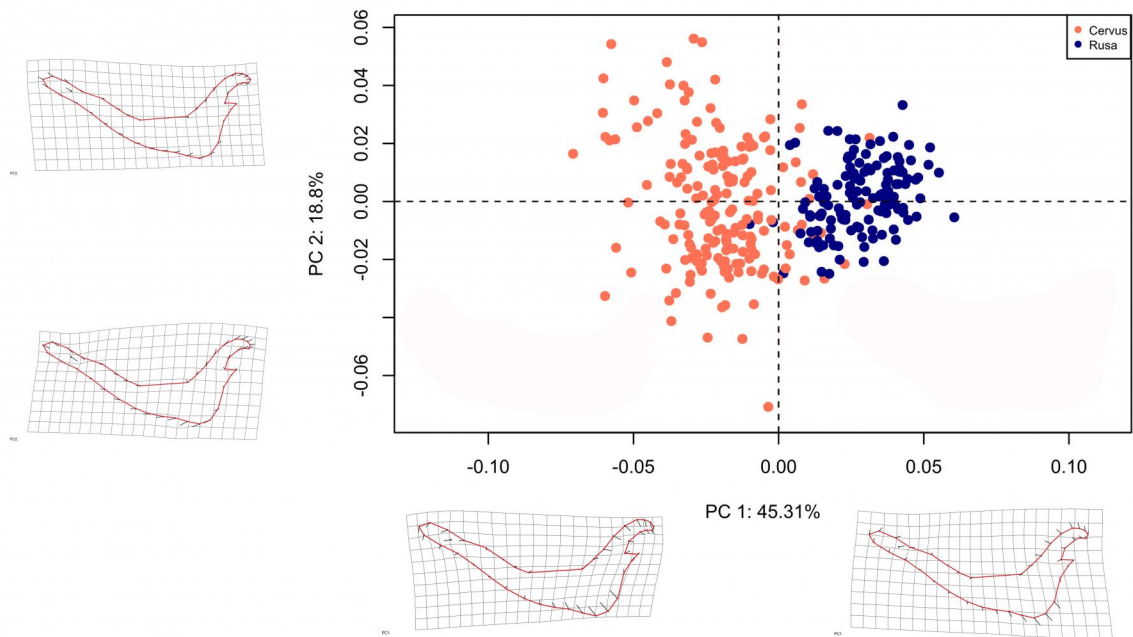
| Landmarks | Names and Description |
|----------------------|--|
| 1 | Tip of the condylar process |
| 2 | Ventral margin of the mandibular sigmoid notch |
| 6 | Ventrocaudal margin of the coronoid process |
| 7 | Tip of the coronoid process |
| 16 | Posterior alveolar margin of <i>M1</i> |
| 17 | Anterior alveolar margin of <i>M1</i> |
| 18 | Posterior alveolar margin of <i>P3</i> |
| 19 | Anterior alveolar margin of <i>P2</i> |
| 22 | Posterior alveolar margin of <i>C</i> |
| 23 | Ventral margin of the <i>I1</i> |
| 25 | Mental foramen |
| 26 | Posterior margin of the mandibular symphysis |
| Semilandmarks | Description traits |
| 3 to 5 | Concavity of the posterior border of the coronoid apophysis |
| 8 to 15 | Convexity of the anterior edge of the coronoid process |
| 20 to 21 | In the mandibular diastema, at the level of the Semilandmark 27 (20) and of the Landmark 25 (21) |
| 24 | Rostro-ventral margin of the horizontal ramus of the mandible, at the level of the posterior alveolar margin of <i>C</i> |
| 27 to 38 | Convexity of the ventral margin of the horizontal ramus of the mandible to the posterior margin of the angular process |
| 38 to 40 | Concavity of the caudal edge of the mandible ramus |



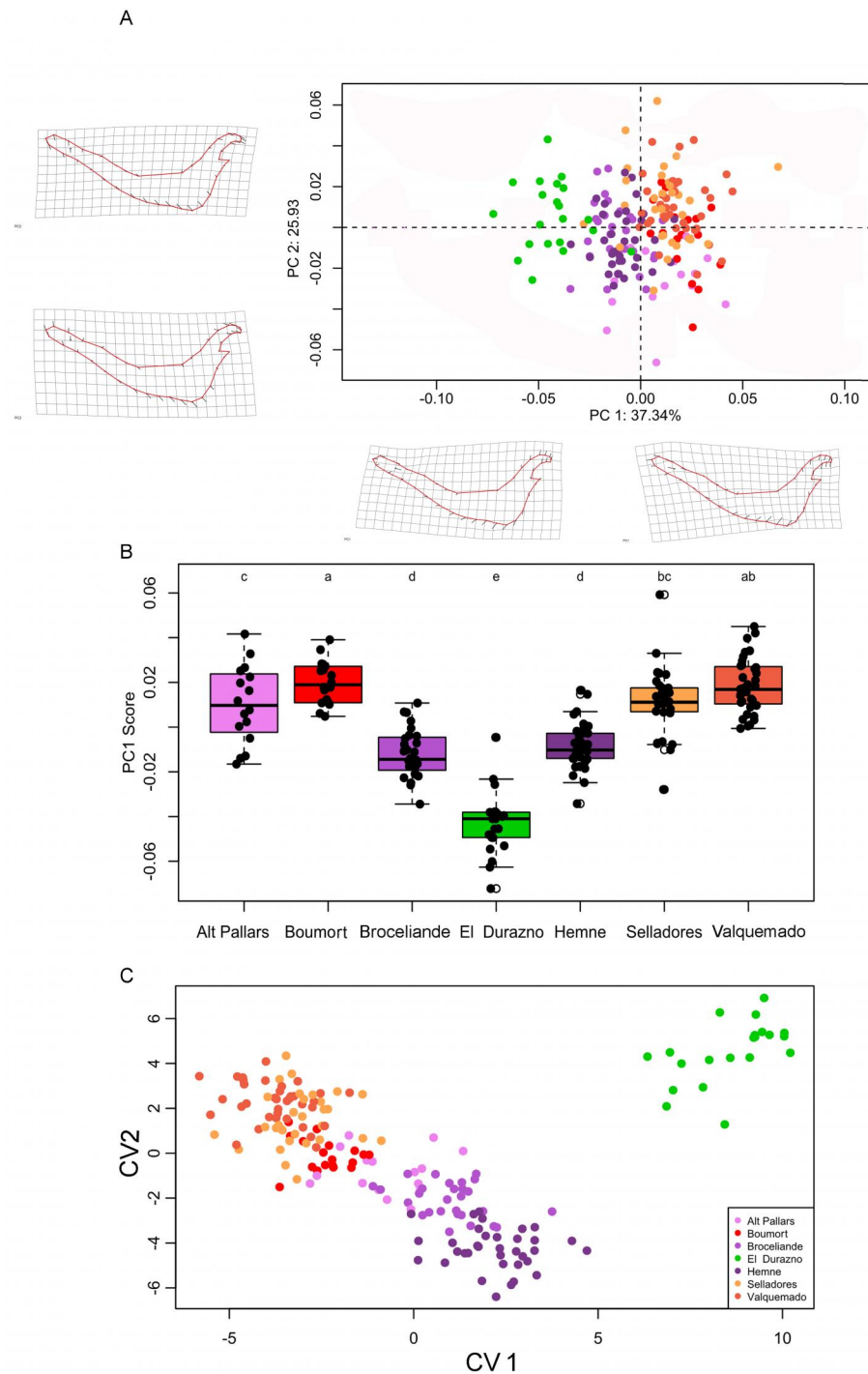
Location of the eight Cervini populations included in the study. *Cervus elaphus*: El Durazno, Hemne, Broceliande, Alt Pallars, Boumort, Selladores, Valquemado. *Rusa timorensis*: New Caledonia (Gouaro Déva, Le Cap, Misère, Parc des Grandes Fougères (PGF)).



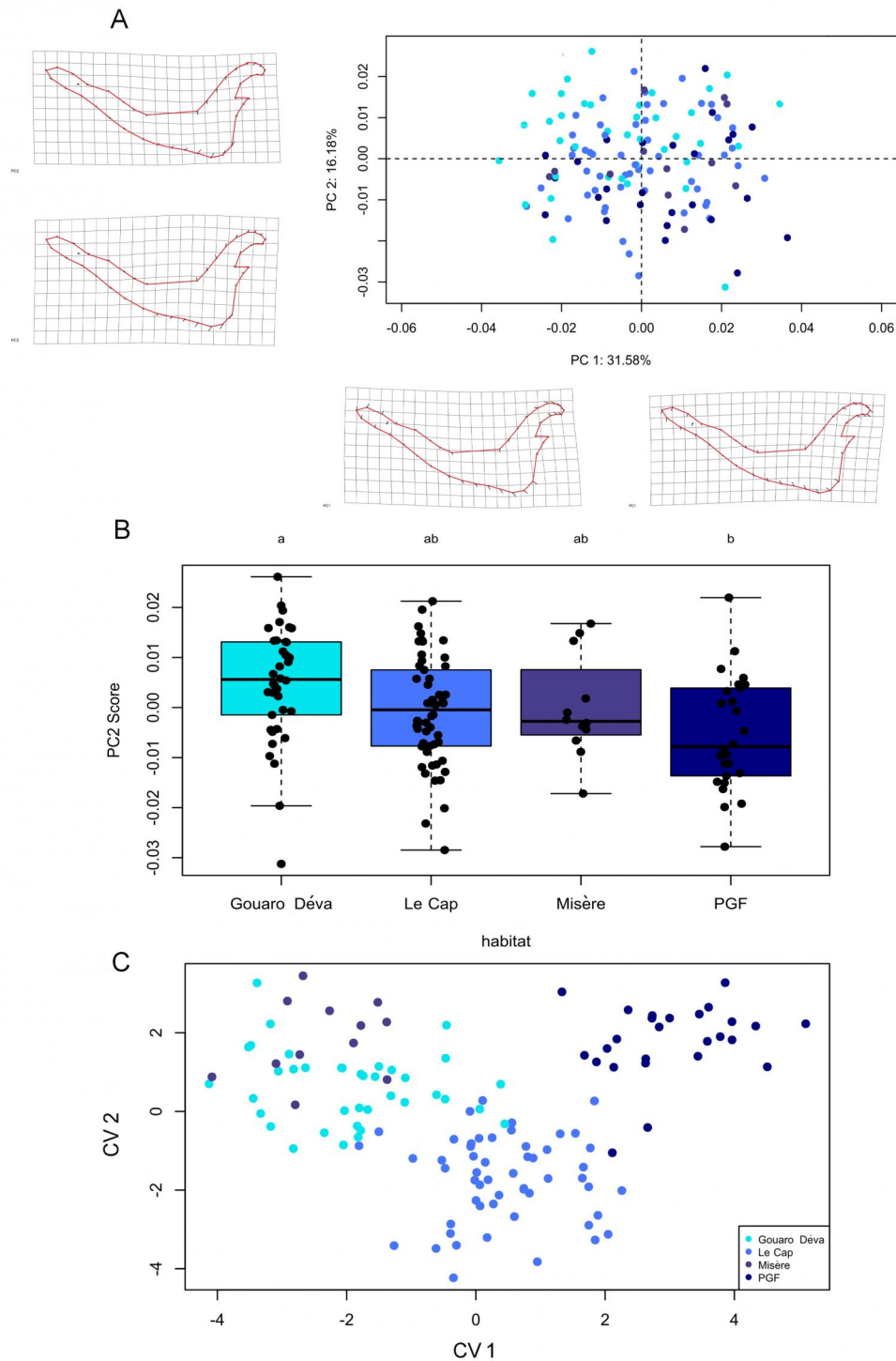
Landmarks (blue) and semi-landmarks (black) used to capture the mandibular bone morphology through a 2D geometric morphometric analysis on the buccal side of the left hemimandible. A: mandible of a red deer specimen from the Selladores-Contadero population. B: Consensus shape for *Cervus elaphus*. The anatomical structures and regions corresponding to numbers 1-40 are described in Table 2.



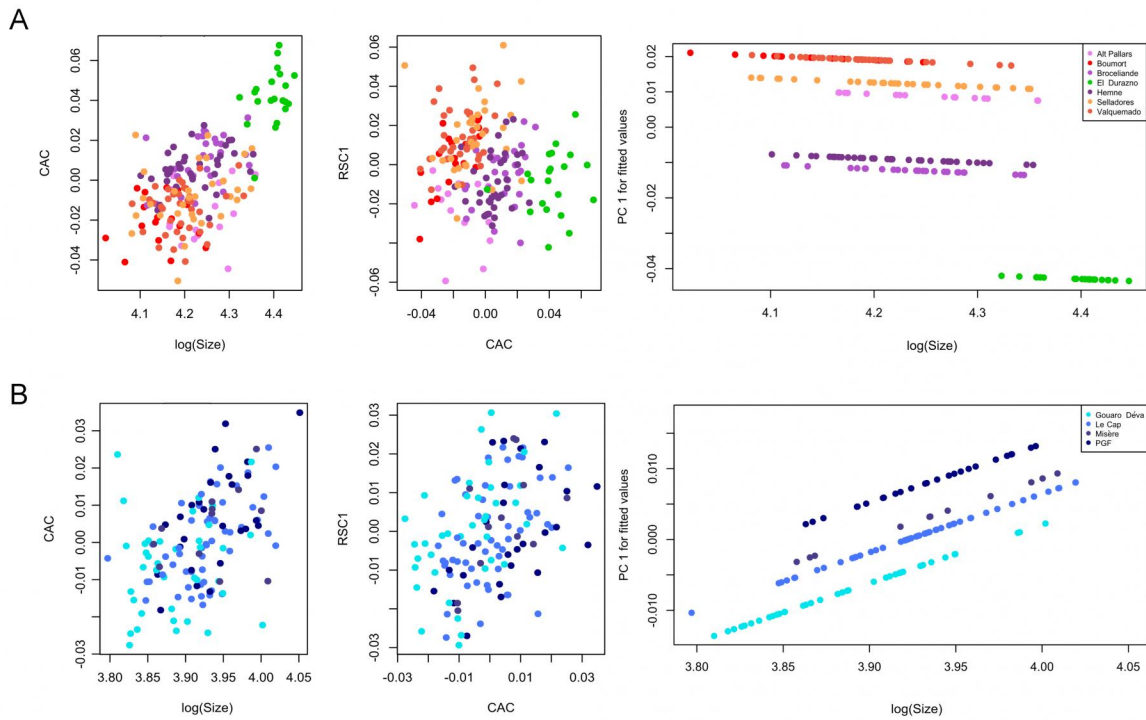
Biplot representing the two first principal components of the PCA exploring interspecific mandibular shape variations between *Cervus elaphus* and *Rusa timorensis*. Shape deformations are shown along PC1 and 2 for each species (*C. elaphus*: coral; *R. timorensis*: navy blue). The consensus shape for all Cervini is shown in grey to aid interpretation.



A: Biplot representing the two first principal components of the PCA (63.3% of the variance) exploring *Cervus elaphus* interpopulation mandibular shape variations. Shape deformations are shown along PC1 and 2 for each population (Alt Pallars: pink; Boumort: red; Broceliande: mauve; El Durazno: green; Hemne: purple; Selladores: dark yellow; Valquemado: orange). The consensus shape for all *C. elaphus* is in grey to aid interpretation. B: Focus on the variation on PC1. Letters (a-e) represent interpopulation differences based on Duncan post hoc test. C: Biplot representing the two first canonical variates of the CVA.



A: Biplot representing the two first principal components of the PCA (47.76% of the variance) exploring *Rusa timorensis* intrapopulation mandibular shape variations between contrasting habitats. Shape deformations are shown along PC1 and 2 for each population (Gouaro Déva: Turquoise, Le Cap: royal blue, Misère: plum, Parc des Grandes Fougères (PGF): navy blue). The consensus shape for all *R. timorensis* is in grey to aid interpretation. B: Focus on the variation on PC2. Letters a and b represent interpopulation differences based on Duncan's post hoc test. C: Biplot representing the two first canonical variates of the CVA.



Allometric relationships and morphological variation in *Cervus elaphus* from different populations (A) and *Rusa timorensis* from contrasted local habitats (B). Plots illustrate body size and shape variations, both within and among Cervini populations, highlighting population-specific morphological trends. Log(Size): log-transformed body size; CAC and RSC1 are morphological metrics. CAC: Common Allometric Component; RSC1: Residual Shape Component 1; PC1: Principal Component 1. The rightmost plots provide information regarding allometry or isometry.

Manuscript body

[Download source file \(3.41 MB\)](#)

Tables

Table 1 - [Download source file \(36.08 kB\)](#)

Information on the habitats of cervid populations. Information on biomes is taken from <https://ecoregions.appspot.com/>. Description of the local vegetation for the populations living in geographical Europe is taken from Ozenda & Borel, 2000. For El Durazno and the Neo-Caledonian localities, the description is based on field observations.

Table 2 - [Download source file \(15.94 kB\)](#)

Description of landmarks and semilandmarks used for capturing the mandibular shape for the geometric morphometric analysis.

Figures

Figure 1 - [Download source file \(1.06 MB\)](#)

Location of the eight Cervini populations included in the study. *Cervus elaphus*: El Durazno, Hemne, Broceliande, Alt Pallars, Boumort, Selladores, Valquemado. *Rusa timorensis*: New Caledonia (Gouaro Déva, Le Cap, Misère, Parc des Grandes Fougères (PGF)).

Figure 2 - [Download source file \(1.21 MB\)](#)

Landmarks (blue) and semi-landmarks (black) used to capture the mandibular bone morphology through a 2D geometric morphometric analysis on the buccal side of the left hemimandible. A: mandible of a red deer specimen from the Selladores-Contadero population. B: Consensus shape for *Cervus elaphus*. The anatomical structures and regions corresponding to numbers 1-40 are described in Table 2.

Figure 3 - [Download source file \(6.55 MB\)](#)

Biplot representing the two first principal components of the PCA exploring interspecific mandibular shape variations between *Cervus elaphus* and *Rusa timorensis*. Shape deformations are shown along PC1 and 2 for each species (*C. elaphus*: coral; *R. timorensis*: navy blue). The consensus shape for all Cervini is shown in grey to aid interpretation.

Figure 4 - [Download source file \(3.03 MB\)](#)

A: Biplot representing the two first principal components of the PCA (63.3% of the variance) exploring *Cervus elaphus* interpopulation mandibular shape variations. Shape deformations are shown along PC1 and 2 for each population (Alt Pallar: pink; Boumort: red; Broceliande: mauve; El Durazno: green; Hemne: purple; Selladores: dark yellow; Valquemado: orange). The consensus shape for all *C. elaphus* is in grey to aid interpretation. B: Focus on the variation on PC1. Letters (a-e) represent interpopulation differences based on Duncan post hoc test. C: Biplot representing the two first canonical variates of the CVA.

Figure 5 - [Download source file \(2.4 MB\)](#)

A: Biplot representing the two first principal components of the PCA (47.76% of the variance) exploring *Rusa timorensis* intrapopulation mandibular shape variations between contrasting habitats. Shape deformations are shown along PC1 and 2 for each population (Gouaro Déva: Turquoise, Le Cap: royal blue, Misère: plum, Parc des Grandes Fougères (PGF): navy blue). The consensus shape for all *R. timorensis* is in grey to aid interpretation. B: Focus on the variation on PC2. Letters a and b represent interpopulation differences based on Duncan's post hoc test. C: Biplot representing the two first canonical variates of the CVA.

Figure 6 - [Download source file \(1.74 MB\)](#)

Allometric relationships and morphological variation in *Cervus elaphus* from different populations (A) and *Rusa timorensis* from contrasted local habitats (B). Plots illustrate body size and shape variations, both within and among Cervini populations, highlighting population-specific morphological trends. Log(Size): log-transformed body size; CAC and

RSC1 are morphological metrics. CAC: Common Allometric Component; RSC1: Residual Shape Component 1; PC1: Principal Component 1. The rightmost plots provide information regarding allometry or isometry.

Supplementary Online Material

File 1 - [Download source file \(166 kB\)](#)

Table S1: results of ANOVA analyses (p-values)

File 2 - [Download source file \(52.45 kB\)](#)

Table S2: results of Duncan post-hoc tests

File 3 - [Download source file \(21.84 kB\)](#)

Table S3: results of procrust regressions evaluating how mandible shape vary as a function of size and species (for Cervini), population (for *C. elaphus*) and habitat (for *R. timorensis*).

File 4 - [Download source file \(31.17 kB\)](#)

Table S4: results of procrust regressions (p-values and R^2) for each axis of PCA carrying significant interpopulation and inter-habitat differences.

File 5 - [Download source file \(22.38 kB\)](#)

Table S5: results of Partial Least Squares

File 6 - [Download source file \(1.52 MB\)](#)

R script (R Markdown)